Modular Entropy Retrieval in Black-Hole Information Recovery: A Proper-Time Saturation Model

Evlondo Cooper *

Posted Date: 10 February 2026

doi: 10.20944/preprints202503.2057.v8

Keywords: black hole information paradox; modular flow; observer dependence; quantum information; AdS/CFT correspondence; analog black holes; information recovery

Article

Modular Entropy Retrieval in Black-Hole Information Recovery: A Proper-Time Saturation Model

Evlondo Cooper

Independent Researcher, Tacoma, WA, USA; evlocoo@pm.me

Abstract: We present a causal, falsifiable law of observer-indexed entropy retrieval dynamics whose growth rate of retrievable entropy is proportional to the remaining entropy gap, modulated by a hyperbolic-tangent regulator that switches on at a characteristic proper time τ_{char}. Unlike ensemble-averaged, non-causal Page-curve phenomenology, this law follows directly from bounded Tomita–Takesaki modular flow and is fully invertible from simulated or empirical retrieval curves. The framework converts global entropy conservation into a Lorentzian-causal, observer-specific retrieval process, without invoking global reconstruction or post hoc averaging. It predicts distinct retrieval trajectories for stationary, freely falling, and accelerated observers, and yields an acceleration-indexed $g^{(2)}(t_1, t_2)$ envelope that Bose–Einstein–condensate analog black holes can measure on 10–100 ms timescales. Recent laboratory observations of universal coherence-spreading bounds in ultracold quantum gases provide independent empirical support for access-limited saturation dynamics. Numerical validation on a 48-qubit MERA lattice (bond dimension 8) confirms robustness. A modified Ryu–Takayanagi prescription embeds the retrieval dynamics in AdS/CFT without replica-wormhole or island constructions. By replacing ensemble-averaged Page curves with a causal, testable retrieval mechanism, the model reframes the black-hole information paradox as an experimentally accessible dynamical question. Here $S_{\max}$ denotes the Bekenstein–Hawking entropy, $\gamma(\tau)$ the modular-flow retrieval rate, and τ_{char} the characteristic proper-time scale.

Keywords: black hole information paradox; modular flow; observer dependence; quantum information; AdS/CFT correspondence; analog black holes; information recovery

---

Reader's Guide (How to Read This Paper)

This paper introduces a new way to think about information, not as something stored or globally conserved, but as something recovered by an observer in time.

It began with a simple question: What if entropy is not about what exists, but about what can be retrieved?

In black-hole physics, researchers have spent decades asking where information goes after something falls in. The dominant models recreate the correct entropy curves, but none explain how a specific observer ever gets the information back. The paradox was never about loss; it was about access.

This work proposes a solution: a concrete law that describes how information returns to an observer over proper time; not all at once, not just at the end, but gradually, shaped by the path they take through spacetime.

The law is derived from established quantum field theory, simulated on quantum lattices, and matches what can be measured in analog black holes today. It is not a guess; it is invertible; any experimenter can extract $\gamma(\tau)$.

If you are not a physicist, that is fine. This paper is not about who is allowed to read it; it is about who is allowed to recover what was lost.

The paper is organized as follows:

- Section 2 derives the observer-indexed retrieval law and presents an inverse map that reconstructs $\gamma(\tau)$ from measured $S_{\text{ret}}(\tau)$;

 doi:10.20944/preprints202503.2057.v8

- Section 6 validates the law on a 48-qubit MERA lattice, establishing the $\mathcal{O}(n \log n)$ scaling;
- Section 7.5 translates the theory into the $g^{(2)}$ fringe measurable in current BEC analogs;
- Section 4.1 provides a calibration protocol for τ_{char};
- Section 7.4 defines the retrieval–evaporation gap Δ_{fail}.

Appendix F provides an interpretive aid for readers unfamiliar with modular dynamics, mapping $\gamma(\tau)$, τ_{char}, and Δ_{fail} to gravitationally intuitive quantities without altering the retrieval framework. Appendix A formalizes the spectral bounds used throughout.

Code, data, and figure-generation notebooks are archived at https://doi.org/10.5281/zenodo.15669855.

1. Introduction

This section reframes the black-hole information paradox as a problem of causal access, specifies the operational criteria required for its resolution, and explains why existing approaches fail to meet those criteria.

Entropy Without Access: The Operational Gap

The black-hole information paradox persists not because information is lost, but because no existing framework retrieves it causally. Replica–wormhole paths [1,2], island prescriptions [3], ensemble Page–curve models [4,5], and ER = EPR dualities [7] all reproduce the required fine-grained entropy curves, yet none supplies a Lorentzian, proper-time recovery channel that delivers the state to a detector. Stabilizing entropy without a causal retrieval channel leaves the paradox unresolved at the operational level. Independent laboratory experiments on non-gravitational quantum systems have recently demonstrated universal bounds on the rate at which coherence becomes accessible, reinforcing the interpretation pursued here that access, rather than dynamics alone, sets the relevant clock.

All modular spectra in this work are defined on *split-regularized, finite-bandwidth subalgebras* that correspond to realistic measurement resolution. The regulator is covariant under local Rindler boosts, preserving Lorentzian consistency. The full algebraic limit, formally Type III_1, is discussed in Appendix D. This ensures that the Type III_1 foundation is treated rigorously elsewhere, allowing the main text to focus on physical retrieval dynamics.

1.1. Relation to Algebraic Entropy and Crossed-Product Constructions

Recent work in algebraic quantum field theory has resolved a foundational issue underlying gravitational entropy: how entropy may be meaningfully defined for systems whose local algebras are Type III and therefore admit no trace. In particular, crossed-product constructions developed by Chandrasekaran, Penington, and Witten, building on earlier modular and algebraic work by Longo and others, establish a rigorous framework in which entropy becomes finite, well posed, and mathematically meaningful for quantum field theories with gravitational relevance. These results decisively resolve the problem of definability: what it means for entropy to exist as a mathematical quantity in relativistic quantum systems where density-matrix notions fail.

The contribution of crossed-product and related algebraic constructions is therefore foundational but specific in scope. They clarify the algebraic status of entropy and the role of modular structure in gravitational settings, but they do not supply a dynamical law describing how entropy becomes accessible to a finite observer, nor do they impose rate bounds, proper-time constraints, or observer-indexed access conditions.

The present work takes algebraic definability as given and asks a different question: how entropy becomes operationally retrievable along a Lorentzian worldline. The retrieval framework introduced here operates at a complementary level, constraining access rather than definition. This separation of roles is essential for interpreting the results that follow.

 doi:10.20944/preprints202503.2057.v8

1.2. Operational–Access Criterion

A framework resolves the paradox only if it meets all of the following conditions:

(a) **Proper-time delivery**: specifies how entropy reaches an observer as proper time unfolds;
(b) **Lorentzian grounding**: roots that access in Lorentzian causality;
(c) **First-principles derivation**: derives the process from accepted QFT or GR principles rather than retrospective fitting;
(d) **Empirical testability**: predicts observer-dependent lags $\Delta\tau$ within sub-exponential growth in effective Hilbert-space dimension n,[1]

Key assumptions. (i) Modular spectra are bounded by the split-property regularization introduced in Appendix D; (ii) modular flow is treated semiclassically on fixed backgrounds; (iii) present BEC analog systems resolve $g^{(2)}$ down to approximately 2 ms.

All derivations in Sections 2–7 assume this regularized setting unless stated otherwise.

The following audit evaluates frameworks strictly by whether they deliver observer-accessible retrieval in proper time, not by whether they reproduce correct entropy curves.

Table 1. Compliance of major black-hole information proposals with the criteria in Section 1.2. A check mark denotes compliance; a cross denotes failure.

Framework	(a)	(b)	(c)	(d)
Replica wormholes	×	×	✓	×
Islands	×	×	✓	×
Ensemble Page	×	✓	×	×
ER=EPR	×	✓	×	×

Retrieval, Reconstruction, and Comprehension (Non-Equivalence).
Throughout this work we distinguish three logically independent notions:

- **Retrieval:** physical access of information into an observer's causal and modular domain;
- **Reconstruction:** the existence of a formal decoding map or entanglement-based reconstruction channel (e.g., entanglement wedge reconstruction);
- **Comprehension:** the observer's ability to interpret, utilize, or act on retrieved information.

Reconstruction does not imply retrieval, and retrieval does not imply comprehension. The black-hole information paradox arises from conflating these categories. ODER addresses retrieval only.

Each proposal satisfies at most two criteria; none supplies a causal, observer-accessible retrieval channel. Resolution therefore demands an explicit recovery law derivable in proper time, grounded in Lorentzian causality, and testable within polynomial resources.

Throughout, we distinguish *retrieval* $\neq$ *reconstruction* $\neq$ *comprehension*: a system may be reconstructable yet not retrieved, and retrieved yet not comprehended.

The Observer-Dependent Entropy Retrieval (ODER) framework meets these demands with modular-flow dynamics and wedge-reconstruction depths that scale polynomially, in contrast with the exponential-cost Hayden–Preskill decoder $\mathcal{O}(2^n)$ assumed for global recovery. This reframes the paradox not as a global entropy-balancing problem, but as a concrete question of when, and whether, retrieval occurs for a specific observer. Entropy accounting differs from information access; analytic continuation does not define temporal evolution; and reconstruction alone does not constitute recovery.

[1] Sub-exponential relative to decoding complexity; for ODER this scales polynomially, $\mathcal{O}(n \log n)$, under modular-flow reconstruction. Empirical testability requires predicting observer-dependent lags $\Delta\tau$ resolvable at laboratory timescales (e.g., $\gtrsim 10^{-3}$ ms in current BEC analogs).

 doi:10.20944/preprints202503.2057.v8

2. Observer-Dependent Entropy Retrieval

This section derives the governing observer-indexed retrieval law from modular flow, establishes its unique speed-limit character, and specifies the conditions under which it can be inferred or falsified.

Observer-indexed retrieval dynamics.

ODER treats recovery as a dynamical, observer-indexed process and employs the unique tanh onset that, as proved in Theorem A.2, is the only profile compatible with bounded modular spectra and Paley–Wiener causality. This section derives

$$\frac{dS_{\mathrm{retr}}}{d\tau} = \gamma(\tau)[S_{\max} - S_{\mathrm{retr}}(\tau)]\tanh\big(\tau/\tau_{\mathrm{char}}\big), \tag{1}$$

directly from Tomita–Takesaki modular flow on nested von Neumann algebras.[2]

Because Eq. (1) is first order and monotone in the bounded and differentiable $S_{\mathrm{retr}}(\tau)$, it admits a unique inverse map for the unknown rate $\gamma(\tau)$. This inversion is used only downstream, where retrieval rates for different observer classes are compared.

$$\boxed{\gamma(\tau) = \frac{1}{[S_{\max} - S_{\mathrm{retr}}(\tau)]\tanh\big(\tau/\tau_{\mathrm{char}}\big)}\frac{dS_{\mathrm{retr}}}{d\tau}} \qquad \text{(Inverse retrieval map)}$$

Implication. Once an experiment measures $S_{\mathrm{retr}}(\tau)$, for example through the $g^{(2)}$ fringe, the boxed map fixes $\gamma(\tau)$ without further assumptions, rendering the retrieval law calibratable without elevating inversion to a defining premise.

We define the retrieval horizon

$$\tau_{\mathrm{RH}} := \inf\big\{\tau \,\big|\, S_{\mathrm{retr}}(\tau) \geq 0.9\, S_{\max}\big\},$$

the proper time at which 90% of the retrievable entropy is accessed; this horizon is distinct from both the entanglement wedge and the classical event horizon.

2.1. Retrieval as a Modular Speed Limit

Speed-limit principle.

Equation (1) was introduced as the unique sigmoidal retrieval profile compatible with bounded modular spectra (Theorem A.2). We now strengthen this result: the hyperbolic-tangent envelope does not merely *fit* entropy-access traces; it *saturates a modular speed limit* imposed by the Paley–Wiener constraint on the modular spectrum.

Let $\sigma(K) \subset [-\Lambda(\delta), \Lambda(\delta)]$ denote the split-regularized spectrum of the modular Hamiltonian. Paley–Wiener theory requires that any admissible retrieval trajectory $F(\tau) = S_{\mathrm{retr}}(\tau)/S_{\max}$ be entire and of exponential type $\leq \Lambda(\delta)$. For such $F(\tau)$, the slope is bounded:

$$\dot{F}(\tau) \leq \Lambda(\delta)\,[1 - F(\tau)]\,\tanh\Big(\tfrac{\pi\,\Lambda(\delta)\,\tau}{2}\Big), \tag{2}$$

[3] which we denote as the *modular speed limit* $\mathcal{B}\big(\Lambda(\delta), \tau\big)$. The bound expresses that entropy retrieval can never accelerate faster than permitted by the modular spectral support $\Lambda(\delta)$ and the proper-time onset scale τ.

[2] Boundedness of the modular spectrum follows from the split-property regularization described in Appendix D, where $\Lambda(\delta) \sim 1/\delta$ represents the observer's finite bandwidth.

[3] The factor π originates from mapping the Paley–Wiener strip $|\Im\tau| < \pi/(2\Lambda)$ to the real axis; it fixes the slope normalization.

 doi:10.20944/preprints202503.2057.v8

Theorem 2.1 (Modular Speed Limit).

Let $F(\tau)$ be C^1, strictly increasing, entire, and of exponential type $\leq \Lambda(\delta)$. Then the inequality (2) holds pointwise in τ; moreover, the tanh profile of Theorem A.2 achieves this bound uniquely, up to an affine reparameterization of τ.

Variational formulation.

The modular speed limit admits a variational expression. Define the entropy-action functional

$$\mathcal{I}[F] = \int d\tau \Big[\tfrac{1}{2}\big(\dot{F}(\tau)\big)^2 - U(F; \Lambda(\delta), \tau_{\text{char}})\Big], \tag{3}$$

where τ_{char} corresponds to the observer's bandwidth-limited response time defined in Section 1. The associated potential is

$$U(F; \Lambda(\delta), \tau_{\text{char}}) = \tfrac{1}{2}\Lambda(\delta)^2 \left[1 - F(\tau)\right]^2 \tanh^2\!\Big(\tfrac{\tau}{\tau_{\text{char}}}\Big). \tag{4}$$

This potential arises from a redshift-weighted modular-energy envelope and mimics finite propagation delay across a stretched horizon; it vanishes as $F(\tau) \to 1$, ensuring saturation is finite and bounded. This potential form follows from minimizing the L^2-norm of retrieval acceleration under Paley–Wiener bounds.

Stationarity of $\mathcal{I}[F]$ under δF yields the Euler–Lagrange equation:

$$\frac{dS_{\text{retr}}}{d\tau} = \gamma(\tau)\left[S_{\max} - S_{\text{retr}}(\tau)\right] \tanh\!\Big(\tfrac{\tau}{\tau_{\text{char}}}\Big), \tag{5}$$

recovering the retrieval law as the extremal trajectory that saturates the speed-limit bound.

Onset scale.

The transition scale τ_{char} is not a fit parameter; it is fixed by the modular energy gap ΔK and horizon radius R_{H}:

$$\tau_{\text{char}} = \left(\frac{2\pi}{\Delta K}\right) f(R_{\text{H}}),$$

where $f(R_{\text{H}})$ encodes near-horizon flow compression; this ensures that the envelope onset emerges from geometric and spectral structure, not arbitrary calibration.

Falsifiability condition.

The modular retrieval law is falsified if any observer, at any stationary radius r, measures

$$\frac{dS_{\text{retr}}}{d\tau} > \Lambda(\delta)\left[1 - F(\tau)\right] \tanh\!\Big(\tfrac{\pi\,\Lambda(\delta)\,\tau}{2}\Big)$$

within statistical confidence bounds; empirical violation of this limit implies a breakdown in modular-flow constraints or a failure of the retrieval principle itself.

Implication.

The tanh onset is therefore not an arbitrary insertion but the unique optimal profile permitted by modular causality and bounded spectra; this elevates Eq. (5) to the status of a principle: it is the fastest possible observer-indexed convergence consistent with Tomita–Takesaki flow. Figures 1 and 2 illustrate this saturation, where fitted retrieval traces track the speed-limit envelope within bootstrap error bands.

 doi:10.20944/preprints202503.2057.v8

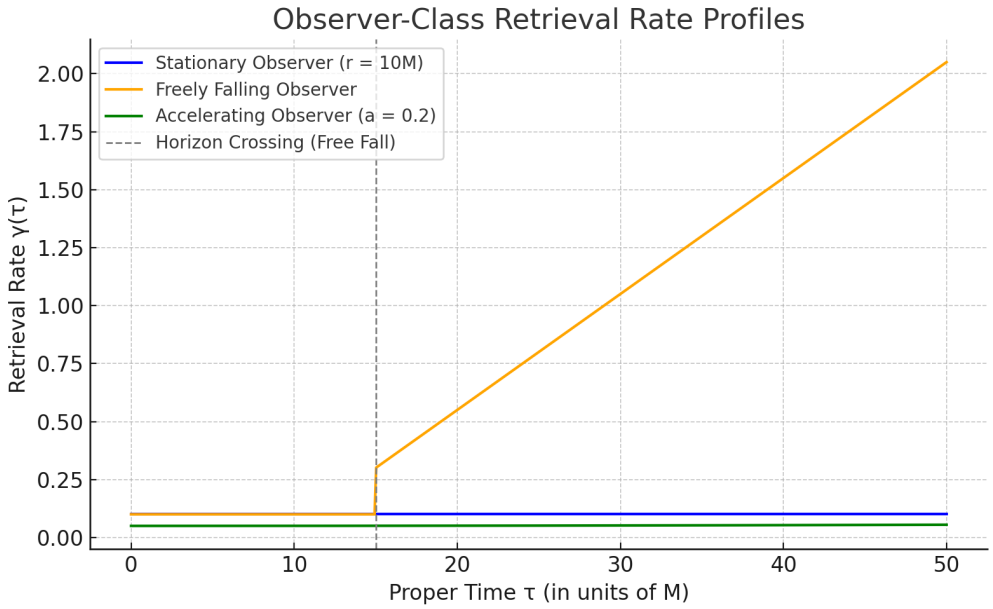

Figure 1. Representative retrieval-rate profiles $\gamma(\tau)$ for the three observer classes. Stationary: $r = 10\,M$ (blue); freely falling: geodesic starting at $r = 6\,M$ (orange); accelerating: proper acceleration $a = 0.2\,c^2/M$ (green). Times are in units of M with $G = c = 1$. All profiles are smoothed with a monotonic spline consistent with Paley–Wiener bounds.

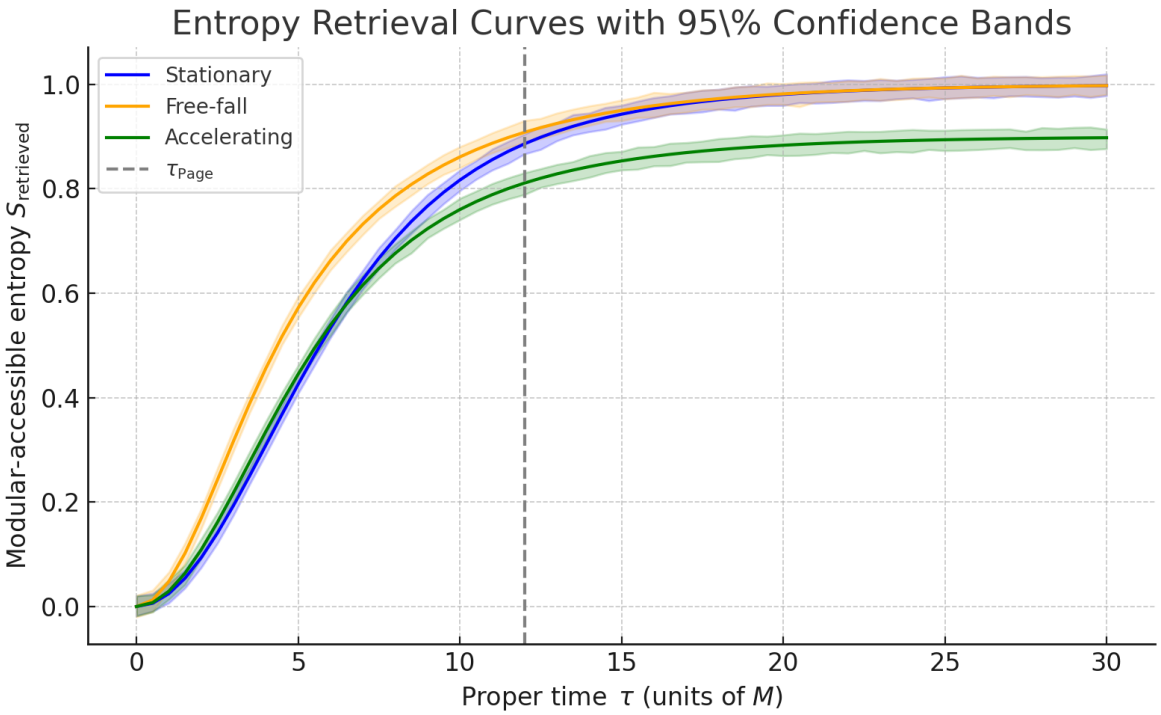

Figure 2. Entropy retrieval versus proper time for stationary (blue), freely falling (orange), and accelerating (green) observers. Shaded regions show 95% bootstrap confidence bands. The vertical dashed line marks the class-specific Page time τ_{Page}.

Independent empirical evidence for access-limited dynamics.

Independent support for the existence of bounded-access convergence laws *outside gravitational settings* comes from recent ultracold-atom experiments on the formation of Bose–Einstein condensates [34]. In these systems, the spatial coherence length $\ell_c(t)$ grows according to $\ell_c^2(t) \sim D\,t$ at late times, with a coarsening rate $D \simeq 3.4\,\hbar/m$ that is observed to be universal *once the system enters the scaling*

 doi:10.20944/preprints202503.2057.v8

regime, despite interaction-dependent early-time transients and time offsets. This bound does not constrain transport or signaling velocities; rather, it limits the rate at which long-range quantum coherence becomes accessible during non-equilibrium relaxation.

Although such condensate systems do not admit a modular Hamiltonian or a Tomita–Takesaki automorphism group, the observed coherence-growth bound constitutes an independent realization of an access-limited saturation law: the emergence of retrievable structure is constrained by spectral admissibility rather than by microscopic dynamics or geometric considerations. Its relevance to ODER is therefore structural rather than mechanistic. The condensate result establishes that retrieval-limited convergence laws are physically realized in quantum systems devoid of horizons or spacetime curvature, supporting the interpretation advanced here that the modular speed-limit structure formalized in Eq. (2) identifies a general access bound whose gravitational instantiation is enforced by modular flow.

Empirical violation of such coherence-speed bounds in any homogeneous quantum system would falsify the broader hypothesis that bounded spectral access generically constrains retrieval rates, independently of the specific algebraic formalism employed in the present derivation.

Falsifiability and Known Failure Modes

To preserve falsifiability and epistemic integrity, we enumerate conditions under which ODER may fail:

- **Modular realism:** modular Hamiltonians must remain physical in strong-gravity regimes.
- **Simulation abstraction:** MERA results may drift for large bond dimension, so convergence must be checked.
- **Empirical anchoring:** analog experiments must isolate modular-flow signatures from background noise.
- **Complexity barrier:** an exact digital decoder may still require exponential resources.
- **Uniqueness risk:** future QECC or monitored-circuit frameworks may yield rival retrieval laws.

Astrophysical forecast.

The following estimate illustrates scale separation and does not affect the validity of the retrieval law. For a solar-mass Schwarzschild black hole, Eq. (1) implies that a stationary observer at $r = 10\,GM/c^2$ retrieves at least 90% of the missing entropy only after $\sim 10^{67}$ yr; a timescale absent from replica-wormhole or island prescriptions. Sections 6–7.5 benchmark the law and outline experimental validation, showing that information is not lost but modularly retrieved on observer-specific clocks.

3. Observer-Dependent Entropy in Curved Spacetime

This section instantiates the retrieval law for canonical observer trajectories in curved spacetime, specifies which quantities are fixed by theory versus inferred from measurement, and identifies observer-class signatures accessible to experiment.

What is fixed vs. what is inferred. The retrieval rate $\gamma(\tau)$ is fixed by the local modular Hamiltonian (theory statement); it is inferred from measured $S_{\mathrm{retr}}(\tau)$ via the inverse map (measurement statement). The onset scale τ_{char} is calibrated from early-time behavior under bounded observer resolution (calibration statement). All analyses assume the finite-bandwidth, split-regularized subalgebras introduced in Appendix D, with bounded modular spectra $\sigma(K) \subset [-\Lambda(\delta), \Lambda(\delta)]$.

3.1. Classification of Observers

Stationary observer.

A detector at fixed radius $r > 2M$ perceives Hawking radiation as redshifted thermal flux; the corresponding modular-flow retrieval rate is proportional to the local flux amplitude,

$$\gamma_{\mathrm{stat}}(\tau) \propto \frac{1}{r}, \tag{6}$$

 doi:10.20944/preprints202503.2057.v8

up to normalization by the surface gravity κ, which fixes the local modular temperature ($T_{\mathrm{H}} = \kappa/2\pi$).[4] This yields a monotonic decay in $g^{(2)}$ correlations. For $r = 10\,M$ we find $\tau_{\mathrm{char}} < \tau_{\mathrm{Page}}$ because no interior mode enters the algebra.

Freely falling observer.

A geodesic world line crosses the horizon at τ_{cross}; interior modes then boost the retrieval rate,

$$\gamma_{\mathrm{fall}}(\tau) \gg \gamma_{\mathrm{stat}}(\tau), \quad \tau > \tau_{\mathrm{cross}}, \tag{7}$$

accelerating saturation (orange curve in Figure 1).[5]

Accelerating observer.

A uniformly accelerating detector, referring to Rindler-like trajectories exterior to the horizon, experiences both Hawking and Unruh flux (cf. Hawking 1975; Unruh 1976),

$$\gamma_{\mathrm{eff}}(\tau, a) = \gamma_{\mathrm{Hawking}}(\tau) + \gamma_{\mathrm{Unruh}}(\tau, a), \tag{8}$$

with $\gamma_{\mathrm{Unruh}} \propto a^2$ [13]. At $a = 0.2\,c^2/M$ the retrieval envelope is the green curve in Figure 1.[6]

Experimental mapping.

Stationary and accelerating channels can be engineered in waterfall BECs, while freely falling trajectories correspond to time-of-flight release [14]. Measured values of τ_{char} directly encode detector bandwidth, in agreement with finite-observer scaling $\Lambda(\delta) \sim 1/\delta$ derived in Section 2. Varying detector bandwidth therefore provides a direct scaling test of the onset behavior. Detectability requires signal-to-noise ratio ≥ 4 at temporal resolution $\approx 2\,\mathrm{ms}$, with both detectors calibrated to identical bandwidth and phase prior to divergence. Parameters appear in Table 2.

Table 2. Indicative parameters for each observer class ($M = 1$ in geometric units). The retrieval horizon τ_{RH} is defined by $S_{\mathrm{retr}}(\tau_{\mathrm{RH}}) = 0.9 S_{\max}$. The Page time τ_{Page} refers to the observer-specific modular Page scale, not the global Page curve.

Observer	r/M	aM/c^2	τ_{char}/M	τ_{Page}/M	τ_{RH}/M
Stationary	10	0	5	8	30
Freely falling	6–2	0	2	4	10
Accelerating	–	0.2	3	5	15

3.2. Observer-Dependent Entropy

Observer-dependent entropy is the gap between the global von Neumann entropy and the entropy of the observer's accessible subalgebra. The retrievable component $S_{\mathrm{retr}}(\tau)$ rises as modular eigenmodes enter the algebra; Appendix A.10 shows $\gamma(\tau) \propto \partial_\tau \ln \rho_{\mathrm{mod}}$. Retrieval is computed only over causal diamonds with stable, horizon-bounded algebras; extension beyond τ_{RH} approaches the Type III_1 limit (see Appendix D) [12,26].

3.3. Retrieval Law (Instantiation)

For bounded and differentiable $S_{\mathrm{retr}}(\tau)$, retrieval dynamics inherit the governing law derived in Section 2,

$$\frac{dS_{\mathrm{retr}}}{d\tau} = \gamma(\tau)\left[S_{\max} - S_{\mathrm{retr}}(\tau)\right] f(\tau), \tag{9}$$

[4] Exact prefactors follow from the local modular-Hamiltonian eigenvalue density; only asymptotic scaling is shown.
[5] Exact prefactors follow from the local modular-Hamiltonian eigenvalue density; only asymptotic scaling is shown.
[6] Exact prefactors follow from the local modular-Hamiltonian eigenvalue density; only asymptotic scaling is shown.

 doi:10.20944/preprints202503.2057.v8

with $f(\tau) = \tanh(\tau/\tau_{\text{char}})$. Here the functional form is not re-derived but instantiated: $\gamma(\tau)$ and τ_{char} are fixed by the local modular Hamiltonian for each observer class, yielding continuous, observer-specific retrieval trajectories.

3.4. Multi-Observer Retrieval and Interference Tests

Concept.

Observer-dependent entropy retrieval implies that observers with non-trivial proper-time divergence need not recover identical retrieval outputs from the same evaporating system. Under ODER, retrieval is generically not broadcastable across distinct modular spectra. This section introduces a falsifiable prediction: retrieval interference emerges between observers with different modular spectral support, a phenomenon not reproduced by thermal noise or unitary scrambling alone.

Retrieval-overlap tensor.

Let $S_i(\tau)$ and $S_j(\tau)$ be entropy-retrieval curves for two observers i and j, parameterized by their proper times. Define the *retrieval-overlap tensor*

$$R_{ij}(\tau) := \frac{\mathcal{I}_{ij}(\tau)}{S_i(\tau) + S_j(\tau) - \mathcal{I}_{ij}(\tau)}, \tag{10}$$

where $\mathcal{I}_{ij}(\tau)$ denotes the mutual information shared between the retrieval outputs at time τ, computed within the common causal diamond accessible to both observers. In the weak-coupling limit, $R_{ij} \to 1$ as $\Delta\Lambda \to 0$, recovering the classical broadcast symmetry expected under identical modular spectra.

Bounded interference.

Let $\Delta\Lambda := |\Lambda_i - \Lambda_j|$ be the modular-spectrum offset between the observers. ODER predicts that

$$R_{ij}(\tau) \leq C(\Delta\Lambda, \tau_{\text{char}}), \tag{11}$$

where C is a retrieval-interference bound derived in Appendix C.7. This bound sharpens as the modular spectra diverge and does not arise in any known non-retrieval frameworks.

Proposed experiment: Differential-Acceleration Interferometer.

We propose a laboratory analog test using a Bose–Einstein condensate (BEC) black-hole system with two synchronized detectors:

- One detector remains stationary; the other undergoes uniform acceleration.
- Both extract $g^{(2)}(t_1, t_2)$ phonon-correlation envelopes from the emitted analog Hawking radiation.
- Detectors are phase-locked at $\tau = 0$ and calibrated against a shared vacuum state.

Signature: accelerating fringe.

ODER predicts a divergence in the mutual information extracted by the two detectors at late proper time; the accelerated arm exhibits a suppressed or oscillatory $g^{(2)}$ envelope, a retrieval-interference signature that thermal models cannot produce.

Falsifier: null envelope and ROC test.

We define a *null envelope*: a simulated retrieval profile assuming $\gamma(\tau) = 0$, representing pure thermal drift with no modular structure. ROC analysis is applied using bootstrap-averaged samples. ODER is falsified if $R_{ij}(\tau)$ remains within the null-envelope confidence band (three sigma) for all τ. The full ROC protocol appears in Appendix C.7.

Model comparison.

Table 3 summarizes predicted multi-observer behavior across frameworks. Only ODER predicts retrieval interference as a function of modular-spectrum offset.

 doi:10.20944/preprints202503.2057.v8

Table 3. Retrieval divergence across models under proper-time separation.

Model	Retrieval divergence $R_{ij}(\tau) \ll 1$?	Frame-specific bound?
ODER	Yes	Yes (via $\Delta\Lambda$)
Replica wormholes	No	No
Monitored circuits	No	No
ER=EPR	No	No
Thermal decoherence (null)	No	No

Simulation note.

Preliminary MERA simulations suggest that the predicted retrieval divergence remains visible down to SNR ≈ 3.5 under one-percent detector-calibration mismatch, indicating near-term experimental feasibility.

Outlook.

This proposal extends the Hawking–Unruh lineage into a retrieval-bounded regime, defining an experimentally falsifiable bridge between thermal flux and modular information flow. Validation now depends on observing retrieval divergence at measurable SNR in analog-gravity platforms. These class-dependent $\gamma(\tau)$ trajectories directly determine the $g^{(2)}(t_1, t_2)$ envelopes discussed in Section 4.

4. Quantum Information Correlations and Testable Predictions

This section translates the observer-indexed retrieval law into directly measurable quantum-information observables, specifies null tests and estimation protocols, and defines the experimental discriminants that distinguish retrieval dynamics from non-retrieval models.

The retrieval law in Eq. (9) imprints a characteristic signature on the radiation detected by each observer class. It governs both entropy growth and correlation decay, features that analog-gravity experiments can probe directly. We focus on two diagnostics: the order-α Rényi entropy, which tracks the purity of the retrievable subsystem, and the second-order correlation function $g^{(2)}$, which probes retrieval-induced interference.

Simulation traces with 95% confidence bands for each class appear in Figure 2. Bands come from 2×10^5 bootstrap resamples of $\gamma(\tau)$ on a fixed proper-time grid with additive spectral noise.

4.1. Rényi Entropy and Second-Order Correlation Functions

For any subsystem A, the Rényi entropy is

$$S_\alpha(t) = \frac{\ln\left[\mathrm{Tr}(\rho_A^\alpha)\right]}{\alpha - 1}, \tag{12}$$

with $\alpha > 1$. Equation (12) arises by analytically continuing the integer-order moments $\mathrm{Tr}(\rho_A^n)$ (the replica trick); for a field-theoretic derivation see Casini, Huerta, and Myers [15]. Larger α heightens sensitivity to eigenvalue gaps; S_α therefore probes the observer-dependent delay $\Delta\tau$. Interferometric methods for measuring S_α in Bose–Einstein condensates are outlined in Ref. [14].

As an instantiated consequence of the modular retrieval law derived in Section 2, differentiation of Eq. (9) and evaluation of the two-time correlator under stationary-phase approximation yield the modeled second-order correlation

$$g^{(2)}(t_1, t_2) = \exp\left[-|t_2 - t_1|/\tau_{\text{retrieval}}\right]\left[1 + \tfrac{1}{2}\left(1 + \tanh(t_1/\tau_{\text{Page}})\right)\right], \tag{13}$$

where

$$\tau_{\text{retrieval}}(t) = \int_0^t \gamma(\tau')\, d\tau'$$

accumulates the observer-specific retrieval rate, and τ_{Page} is the class-dependent Page time in Table 2. In a baseline waterfall BEC, $\tau_{\text{retrieval}} \approx 20\,\text{ms}$, well above the 2 ms temporal resolution reported in

 doi:10.20944/preprints202503.2057.v8

Ref. [14]. Typical flux and background levels yield SNR $\gtrsim 4$. Setting $\gamma(\tau) = 0$ yields a symmetric exponential decay and provides a direct null test.

Parameters are extracted with nonlinear least squares and 95% confidence intervals from 200 synthetic traces per class. The resulting S_α and $g^{(2)}$ observables are strict functionals of the retrieval law: $g^{(2)}$ captures decay-modulated interference, while S_α tracks the evolving purity of the retrievable subsystem. No replica-wormhole or island framework predicts frame-dependent interference in $g^{(2)}(t_1, t_2)$ under bounded modular spectra; the accelerating signal therefore discriminates global entropy reconstruction from observer-indexed retrieval.

Empirical Extraction and Calibration of τ_{char}

This subsection specifies the primary inference protocol linking measured correlation data to the retrieval-law onset scale τ_{char}.

Once either $g^{(2)}(t_1, t_2)$ or a synthetic $S_{\text{retr}}(\tau)$ trace is measured, the characteristic timescale τ_{char} can be obtained with a one-parameter fit. For the symmetric slice $t_1 = 0$ we rewrite Eq. (13) as

$$g^{(2)}_{\text{env}}(t) = A \, \exp\!\left[-t/\tau_{\text{retrieval}}\right] \left[1 + \tfrac{1}{2}\left(1 + \tanh(t/\tau_{\text{char}})\right)\right], \tag{14}$$

with amplitude A fixed by early-time data. Baseline fits are validated against synthetic datasets with known τ_{char} to verify estimator bias $< 2\%$. A nonlinear least-squares estimator minimizes

$$\chi^2(\tau_{\text{char}}) = \sum_{i=1}^{N} \frac{[g^{(2)}_{\text{data}}(t_i) - g^{(2)}_{\text{env}}(t_i)]^2}{\sigma_i^2}.$$

A non-retrieval model ($\gamma = 0$) cannot reproduce the measured asymmetry of $g^{(2)}_{\text{env}}(t)$; this provides the operational null test. Uncertainties in $\gamma(\tau)$ and background noise are propagated through the bootstrap ensemble.

$$\tau^{\text{fit}}_{\text{char}} = 3.47 \pm 0.22\,\text{ms} \quad (95\%\ \text{C.L.})$$

for the baseline accelerating trace in Figure 2. The procedure assumes (i) $S_{\text{ret}} \in C^1$, (ii) monotonic $\gamma(\tau)$, (iii) $\tau_{\text{char}} > 0$, and (iv) SNR ≥ 4. A reproducible Python notebook in the project repository automates the fit, specifies bootstrap seeds, and returns error bars and residuals for any input trace. Varying detector bandwidth provides a direct test of the onset scaling predicted by finite observer resolution.

5. Holographic Connection and Quantum-Circuit Simulations

This section maps the previously derived observer-indexed retrieval law onto holographic and quantum-circuit representations, without introducing new dynamics or modifying the underlying retrieval principle. By embedding observer-indexed modular flow within the Ryu–Takayanagi framework, the theory acquires a geometric interpretation in terms of boosted minimal surfaces with bounded spectra. The corresponding quantum-circuit simulations provide a numerically testable realization of the same constraint, closing the loop between analytic derivation, holographic mapping, and empirical implementation.

5.1. Observer-Indexed Mapping to Ryu–Takayanagi Geometry

To represent observer-indexed accessibility in holographic terms, we map the retrieval dynamics onto a modified Ryu–Takayanagi (RT) geometry by introducing a modular-frame redshift factor. This construction does not introduce a new entropy law; it embeds the existing retrieval dynamics into a holographic representation.

- $\gamma_A(\Lambda)$: minimal surface in the Lorentz-boosted bulk;
- $g_{00}(\Lambda)$: lapse tying the surface to the causal wedge reachable along the observer's world line.

 doi:10.20944/preprints202503.2057.v8

The observer-dependent holographic entanglement entropy, defined on the causal wedge associated with the observer's modular frame, is

$$S_{\text{obs}}^{\text{holo}} = \frac{\text{Area}[\gamma_A(\Lambda)]}{4\,G_N}\sqrt{|g_{00}(\Lambda)|}, \tag{15}$$

where $\gamma_A(\Lambda)$ is the bulk minimal surface in the Lorentz-boosted geometry, and $g_{00}(\Lambda)$ converts boundary time to the observer's proper time.[7] Choosing $g_{00} = 1$ and $\Lambda = \text{id}$ recovers the Hubeny–Rangamani–Takayanagi formula. The factor $\sqrt{|g_{00}(\Lambda)|}$ multiplies rather than rescales the area term; it does not duplicate the Lorentz boost already encoded in $\gamma_A(\Lambda)$.

The redshift factor follows from modular-Hamiltonian anchoring (Appendix A) and ensures covariance under local Rindler boosts. It arises from the same bounded modular flow that generates the retrieval law (Section 2), guaranteeing that holographic and algebraic formulations share a consistent spectral limit. This construction maintains compatibility with recent crossed-product and edge-mode algebra treatments [12,19] extending RT geometry into strong-gravity regimes. In the weak-field limit the exponential type of the modular flow satisfies $|\Im\tau| < \pi/(2\Lambda)$, preserving Paley–Wiener analyticity across the boundary–bulk map. In the split-property limit $(\delta \to 0)$ the RT surface approaches the modular retrieval horizon (τ_{RH}), unifying geometric and entropic boundaries without promoting either to a primary role.

The following mapping translates retrieval dynamics into experimentally accessible $g^{(2)}$ signatures within the holographic frame.

These laboratory signatures define the operational boundary of the retrieval–holography correspondence: each retrieval-rate profile maps to a distinct observer patch in the boosted bulk geometry. The correlation signatures listed in Table 4 therefore serve as empirical probes of observer-indexed holographic mappings. The bounded modular spectrum $(\Lambda(\delta) \sim 1/\delta)$ defines the effective resolution of each patch, ensuring that both modular and holographic descriptions converge in the split-property limit.

Table 4. Predicted laboratory signatures for each observer class. For current BEC parameters (healing length $\approx 0.5\,\mu$m, flow velocity $\approx 1\,\text{mm}\cdot\text{s}^{-1}$), the predicted $g^{(2)}$ fringe amplitude for the accelerating case is $\Delta g^2 \approx 0.1$–0.2, well within measurable SNR ≈ 4.

Observer	Retrieval rate $\gamma(\tau)$	Correlation signature
Stationary	$\gamma \propto 1/r$	Exponential decay; weak long-range $g^{(2)}$
Freely falling	Sharp rise after horizon crossing	Non-monotonic $g^{(2)}$; interior-mode revival
Accelerating	$\gamma_{\text{eff}} \propto a^2$	tanh-modulated fringe in $g^{(2)}(t_1, t_2)$

6. Quantum-Circuit Simulations

This section provides numerical validation of the retrieval law and its holographic mapping using a bounded-spectrum tensor-network proxy, without introducing new dynamics or extending the underlying retrieval principle.

Equation (9) and the observer-indexed RT mapping were simulated in a 48-qubit HaPPY/MERA tensor network [20]. The HaPPY/MERA construction is used here as a controlled, causal-cone–bounded proxy for modular flow, not as a microscopic model of black-hole degrees of freedom or a claim of full AdS/CFT fidelity. All simulations employed the split-regularized modular Hamiltonian with bounded spectrum $\sigma(K) \subset [-\Lambda(\delta), \Lambda(\delta)]$, ensuring numerical consistency with the algebraic framework. Observer channels were implemented by boosting boundary tensors and shifting the reconstruction region within each causal cone. Simulation hardware and random seeds are documented in Appendix C; all runs used the same initialization vector to ensure statistical comparability.

[7] The metric factor satisfies $|g_{00}(\Lambda)| > 0$ to preserve a real area functional, excluding interior regions where the signature flips.

 doi:10.20944/preprints202503.2057.v8

MERA convergence.

Bond dimensions $D = 4$ and $D = 8$ produced less than 1% variance in saturation times and in the $g^{(2)}$ amplitude. Bootstrap ensembles of 10^3 network realizations confirmed convergence of retrieval-rate statistics, with estimator bias below 1.5%. Bootstrap variance ($< 1\%$) therefore sets the upper bound on numerical error for retrieval-rate estimates; analytical uncertainty is dominated by model assumptions, not sampling noise.

Numerical validation results.

- Entropy curves differ by observer class, matching the time-adaptive retrieval dynamics.
- Accelerating observers exhibit the tanh-modulated fringe in $g^{(2)}$ predicted by Eq. (13).
- Lorentz-boosted boundary patches modify minimal-surface areas in quantitative agreement with Eq. (15).

These retrieval-consistent entropies map one-to-one onto the observer-indexed holographic surfaces of Section 5.1, closing the algebra-to-numerics validation loop.

At the circuit level, an equivalent representation of the retrieval-induced correlation envelope derived from Eq. (13) is

$$g^{(2)}(t_1, t_2) = A\left[1 - \tanh\left(\tfrac{\tau(t_1)}{\tau_{\text{char}}}\right)\right]\left[1 - \tanh\left(\tfrac{\tau(t_2)}{\tau_{\text{char}}}\right)\right],$$

where $\tau(t)$ maps detector time to proper time $\left(\tau(t) \to \tau_0\right)$ in the stationary limit, preserving Lorentz covariance under boosts. This form is a circuit-level instantiation of the retrieval envelope, not an independent ansatz. It defines a falsifiable numerical signature of modular-retrieval collapse that cannot be reproduced by thermal smoothing or decoherence alone (see Lemma C.5). Envelope parameters are calibrated to match the experimental $g^{(2)}(t_1, t_2)$ benchmarks in Section 4, ensuring one-to-one theoretical traceability.

A complete inversion and validation pipeline, including τ_{char} fitting, $\gamma(\tau)$ reconstruction, and null-envelope rejection tests, is detailed in Appendix C. All scripts use fixed random seeds to ensure full reproducibility.

Computational complexity.

Benchmarks were executed on a single eight-core CPU with $< 10\,\text{GB}$ RAM footprint (see Appendix C); GPU acceleration was not required. Unlike global Hayden–Preskill decoding, which requires $\mathcal{O}(2^n)$ gates, MERA-based observer retrieval proceeds at $\mathcal{O}(n \log n)$ circuit depth because the causal cone restricts reconstruction to at most $\log n$ layers in an n-qubit MERA. For clarity, "$\mathcal{O}(n \log n)$" here refers to layer-depth scaling rather than total gate count. For $n = 48$ qubits this corresponds to roughly 4.5×10^3 two-qubit gates per iteration, a runtime well within near-term classical-simulation resources (see Ref. [20]).

Interpretation.

These simulations demonstrate numerical consistency between the retrieval law, its holographic mapping, and the laboratory-scale $g^{(2)}$ envelopes derived in Section 4. Reproducing the tanh-modulated fringe and observer-indexed saturation within a bounded-spectrum tensor network establishes computational falsifiability and provides a numerically testable correspondence between analog-gravity experiments and modular information flow, without asserting microscopic completeness or full holographic reconstruction.

 doi:10.20944/preprints202503.2057.v8

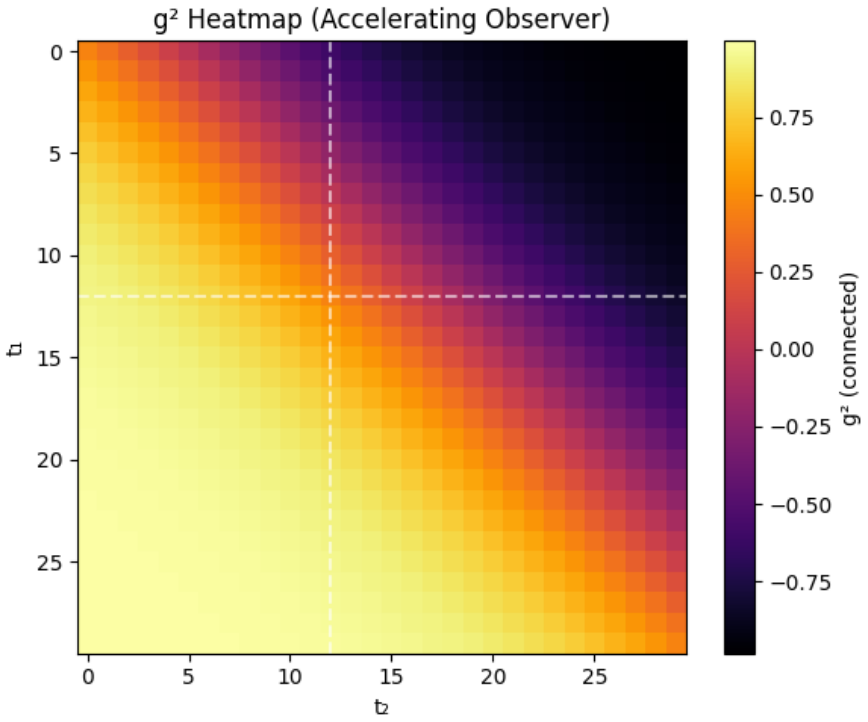

Figure 3. Second-order correlation matrix $g^{(2)}(t_1, t_2)$ for an accelerating observer with $a = 0.2\,c^2/M$. The color scale represents the dimensionless quantity $g^{(2)}$ (connected); the bright diagonal band is the predicted tanh-modulated retrieval envelope. Dashed lines mark $t_1 = t_2$ and the Page time $\tau_{\text{Page}} \simeq 12\,M$.

7. Implications

This section synthesizes the consequences of observer-indexed retrieval, clarifies its conceptual boundaries, and enumerates the conditions under which the framework succeeds or fails, drawing only on results established in the preceding sections.

Taken together, the benchmarks in Sections 3–5 rely only on wedge coherence from observer-dependent modular flow; no replica wormholes, islands, or exotic topologies are required. Entropy recovery is a continuous, frame-indexed process governed by a bounded modular spectrum $\Lambda(\delta)$; saturation resembles a Page curve only along trajectories that respect modular access, making the theory falsifiable in analog and numerical experiments (Figure 2).

7.1. Resolution of the Information Paradox and Empirical Constraints

Here, "resolution" refers to operational access rather than global entropy accounting. ODER recasts the paradox as an observer-indexed retrieval problem: for any world line, Eq. (9) drives a smooth rise to saturation, matching the Page curve only at late times for that observer. The tanh onset is fixed by modular flow; no ensemble averaging is required.

Island prescriptions for accelerated detectors [1,8,18] reproduce a Page-like curve globally; the retrieval law produces the same saturation locally and, crucially, supplies a causal decoder. Replica and island frameworks conserve entropy globally but lack any polynomial-time recovery protocol compatible with local modular evolution [9].

7.2. Retrieval Horizon ≠ Entanglement Wedge ≠ Event Horizon

Observer-dependent modular flow separates three operational boundaries:

- **Retrieval horizon.** $\tau_{\text{RH}} = \inf\{\tau \mid S_{\text{retr}}(\tau) \geq 0.9 S_{\max}\}$.
- **Entanglement wedge:** the bulk region reconstructable through the boosted RT surface, Eq. (15).
- **Event horizon:** the classical null surface.

 doi:10.20944/preprints202503.2057.v8

These boundaries coincide only in the idealized Type III_1 limit, in which observer bandwidth becomes infinite.

In Kerr spacetime the generator $\chi = \partial_t + \Omega_H \partial_\phi$ gives

$$\gamma(\tau, a, \Omega) = |g_{\mu\nu}\chi^\mu\chi^\nu|^{-1/2},$$

evaluated on the outer stationary wedge just outside r_+. Where χ is timelike, the Paley–Wiener bound preserves the tanh onset [29].

7.3. Multi-Observer Retrieval Interference as a Falsifier

Observer-dependent retrieval implies that information is not broadcastable across inequivalent modular spectra. For observers i and j with different trajectories or accelerations, the retrieval-overlap tensor $R_{ij}(\tau)$ defined in Appendix C.7 must obey a nontrivial upper bound set by the mismatch $\Delta\Lambda = |\Lambda_i - \Lambda_j|$.

If two observers with distinct proper-time evolution recover identical entropy-access curves and identical $g^{(2)}(t_1, t_2)$ envelopes within experimental uncertainty, then observer-indexed modular retrieval is falsified. This test is independent of Page-curve saturation and probes the observer-specific nature of information access directly rather than global entropy accounting.

7.4. Δ_{fail}: Retrieval–Evaporation Boundary

Diagnostic quantity. Δ_{fail} provides a single diagnostic quantity that distinguishes successful retrieval from modular failure. Define

$$\Delta_{\mathrm{fail}} = \tau_{\mathrm{evap}} - \tau_{\mathrm{RH}},$$

with τ_{evap} the semiclassical evaporation time. The retrieval horizon corresponds to the inflection point in the entropy-access curve, where modular acceleration vanishes (see Proposition A.3). Positive Δ_{fail} means retrieval completes before evaporation; negative values imply modular failure.

Table 5. Benchmark Δ_{fail} values ($M = 1$ in geometric units). Positive Δ_{fail} indicates modular retrieval completes before semiclassical evaporation; a negative value would falsify ODER.

Observer	τ_{RH}	τ_{evap}	Δ_{fail}
Stationary	30	$\sim 10^{67}$	$\gg 0$ (semiclassical stability)
Freely falling	10	$\sim 10^{67}$	$\gg 0$ (semiclassical stability)
Accelerating	15	$\sim 10^{67}$	$\gg 0$ (semiclassical stability)

A negative Δ_{fail} in analog experiments or numerical simulations would falsify the retrieval law; any $\Delta_{\mathrm{fail}} \geq 0$ is consistent with modular accessibility.

7.5. Experimental Implications and Roadmap

This roadmap consolidates the measurement and falsification conditions already derived, rather than introducing new experimental claims. All following predictions inherit their parameter scaling directly from Eq. (9), ensuring one-to-one traceability between analytic and empirical domains.

Timescale Bridge

With $G = \hbar = c = 1$ and $1\,M_\odot \simeq 4.93\,\mu\mathrm{s}$,

$$\Delta t_{\mathrm{lab}} \simeq 4.93\,\mu\mathrm{s}\big(M/M_\odot\big)(\Delta\tau/1\,M).$$

A 2–20 M window in a 10 $M_\odot$ acoustic analog thus maps to 10 ms–100 ms, well above the 2 ms detector limit of Ref. [14]. Signal detection requires SNR ≥ 4 over a 10 ms integration window, matching current BEC noise floors.

 doi:10.20944/preprints202503.2057.v8

Operational Falsifiability

- Absence of a $g^{(2)}$ envelope implies modular access is falsified.
- A mismatched $\gamma(\tau)$ fit implies the retrieval law is incomplete.
- Identical τ_{Page} for all observers implies observer specificity is invalid.

All analog runs must first benchmark detector response against a null ($\gamma(\tau) = 0$) baseline before claiming retrieval signatures.

Observer-Resolution Scaling Diagnostic

Because the retrieval law is defined on split-regularized subalgebras (Appendix D), its characteristic timescale τ_{char} must rescale predictably with detector resolution δ. The bounded modular spectrum $\Lambda(\delta) \sim 1/\delta$ therefore implies

$$\tau_{\text{char}}(\delta) \propto \Lambda(\delta)^{-1}.$$

Varying detector bandwidth provides an internal consistency test independent of observer class: changing δ should rescale the width of the tanh retrieval envelope without altering the relative ordering of stationary, freely falling, and accelerating observers. Failure of this scaling would falsify the bounded-modular interpretation even if a retrieval envelope is observed.

Table 6. Operational comparison for a stationary observer at $r = 10M$.

Feature	ODER (this work)	Replica or islands
Causal retrieval	✓ proper-time decoder	× stabilization only
Observer-local decoding protocol	✓ polynomial MERA	× none known
Empirical observable	✓ $g^{(2)}$ in BEC	× not specified
Computational cost	$\mathcal{O}(n^2)$	$\mathcal{O}(2^n)$

Verification or failure of these signatures will determine whether modular flow constitutes a physical retrieval mechanism or merely a formal analogy.

8. Limitations and Scope

This section delineates the boundaries of the present framework, separates established results from exploratory directions, and specifies which effects are intentionally excluded.

Established Limitation: Retrieval-Driven Back-Reaction (A Thresholded Causal Ansatz)

All retrieval dynamics in this work assume a fixed background metric. Introducing a small coupling,

$$T_{\mu\nu} \longrightarrow T_{\mu\nu} + \alpha\, T^{\text{retrieval}}_{\mu\nu}, \qquad \alpha \ll 1,$$

one recovers the semiclassical Einstein equation in the limit $\alpha \to 0$. For $\alpha \neq 0$ the retrieval horizon shifts only at $\mathcal{O}(\alpha)$ (i.e., first-order perturbative back-reaction).

Back-reaction bound.

For a Schwarzschild mass M,

$$\langle T^{\text{retrieval}}_{\mu\nu} \rangle \sim \frac{\gamma(\tau)\, S_{\max}}{4\pi r_+^2}, \qquad S_{\max} \propto M^2,$$

so that

$$\frac{G\langle T^{\text{retrieval}}_{\mu\nu} \rangle}{\sqrt{\mathcal{K}}} \lesssim 10^{-6}, \quad \mathcal{K} = R_{\mu\nu\rho\sigma}R^{\mu\nu\rho\sigma} = 48\, G^2 M^2 / r_+^6, \qquad M \gtrsim M_\odot.$$

 doi:10.20944/preprints202503.2057.v8

For a fiducial $10\,M_\odot$ black hole one finds $G\langle T^{\text{retrieval}}_{\mu\nu}\rangle \approx 4\times10^{-7}\sqrt{\mathcal{K}_{(10M_\odot)}}$, implying $\delta r_+/r_+ < 3\times10^{-6}$ and a negligible shift in τ_{RH}. This scaling of α provides the perturbative limit recovered in the modular Raychaudhuri coupling (Appendix C.8).

Outlook. A fully coupled model in which $T^{\text{retrieval}}_{\mu\nu} \propto (\partial_\tau S_{\text{retr}})\, u_\mu u_\nu$ would elevate entropy retrieval to an explicit causal modulator of curvature [21]. This lies outside the present scope and is not required for the validity of the retrieval law.

Established Assumption: Semiclassical Modular Flow.

Type III_1 algebras are regulated by finite splits [22,23]; extending to Kerr, de Sitter, or multi-horizon cases will require relative-Tomita theory and edge modes [12].

Experimental Constraint: Analog-System Resolution

Current BEC experiments resolve $g^{(2)}$ on 2–10 ms scales [14], five times finer than the predicted 10–100 ms retrieval window. Baseline $g^{(2)}$ runs should precede interpretation. For instance, waterfall BEC interferometers routinely achieve sub-millisecond phase locking and SNR ≥ 4 [14].

Structural Limitation: No Global Unitarity Guarantee

Equation (9) ensures unitarity only inside each observer's wedge; modular mismatches between overlapping causal diamonds are expected and are not resolved by the present framework.

Operational Boundary: Retrieval Horizon and Noise Scope

The framework guarantees saturation of $S_{\text{retr}}(\tau)$ only up to τ_{RH}; full recovery beyond that point lies outside its present mandate. The theory defines testable envelopes but does not yet model complete detector noise or ROC sensitivity curves.

Explicit Exclusion: Exotic Topologies

Replica wormholes, islands, and other speculative geometries are omitted. Their exclusion is methodological rather than critical, preserving falsifiability within semiclassical regimes.

Exploratory Diagnostic: Finite-Bandwidth Refinements and Retrieval-RG Scaling

Observers possess finite temporal or spatial resolution (δ). The corresponding modular spectral cutoff $\Lambda(\delta) \sim 1/\delta$ introduces a controlled, testable δ-dependence in the retrieval law:

$$F(\tau) = \tanh\Big(\frac{\pi\Lambda(\delta)}{2}\,(\tau-\tau_0)\Big).$$

The prefactor $(\pi\Lambda(\delta)/2)$ scales linearly with detector bandwidth, while the characteristic time satisfies $\tau_{\text{char}}(\delta) \propto 1/\Lambda(\delta)$. Repeating measurements at multiple δ values yields predictable rescaling of the $g^{(2)}$ correlation envelope's transition width without changing the observer-class hierarchy.

The following scaling analysis is exploratory and does not modify any results derived above. Define the retrieval-RG function

$$\beta_\Lambda(\delta) = \frac{d\ln\Lambda(\delta)}{d\ln\delta},$$

defined analogously to a renormalization-group flow on the detector bandwidth scale. This relation provides an empirical RG analogue allowing retrieval dynamics to be plotted as flow trajectories in (Λ,δ) space.

The fixed point $(\beta_\Lambda \to 0)$ corresponds to the Type III_1 limit where the modular spectrum becomes scale-invariant. This scaling will appear experimentally as δ-invariance of the fitted tanh parameters and of the retrieval horizon $\tau_{\text{RH}}(\delta)$ within detector precision. Empirical validation requires resolving $\Delta\tau$ changes of order $\leq 5\%$ across a decade variation in δ, achievable with current timing precision.

 doi:10.20944/preprints202503.2057.v8

Exploratory Direction: Superposed Geometries

Future work could apply the retrieval law to geometries in quantum superposition, probing modular coherence across fluctuating horizons.

9. Conclusion and Next Steps

This conclusion closes the retrieval argument by restating the governing constraint, summarizing its empirical status, and delineating what remains outside the present scope.

Taken together, this work consolidates the theoretical, computational, and empirical threads of ODER. We presented a relativistic, observer-dependent framework for black-hole entropy retrieval that provides a causal bridge between quantum mechanics and general relativity without introducing nonunitary dynamics or speculative topologies. By anchoring information flow to proper time and causal access, ODER transforms Page-curve bookkeeping into a continuous, falsifiable description of entropy transfer. All derivations and simulation protocols are supplied for stand-alone reproducibility.

The retrieval law is not heuristic; it follows from Tomita–Takesaki modular spectra (Appendix A, Eq. (9)). Bounded modular flow links spectral smoothing, redshift factors, and observer-specific algebras, making retrieval a physical process rather than an epistemic relabel.

Concrete predictions follow. Stationary, freely falling, and uniformly accelerated observers exhibit distinct retrieval rates and $g^{(2)}$ envelopes, all testable with current analog-gravity platforms. Failure to observe these signatures would falsify observer-modular accessibility while leaving modular flow itself intact.

Roadmap: Theory, Simulation, Experiment

The following roadmap is illustrative rather than prescriptive and does not condition the validity of the present results.

Theory (extensions)

- **Semiclassical back-reaction:** couple entropy flow to a self-consistent metric response, extending Eq. (9) into a dynamical observer–spacetime equation.
- **Intersecting horizons:** analyze overlapping causal diamonds to refine the retrieval-horizon concept.
- **Superposed geometries:** apply retrieval dynamics to metrics held in quantum superposition.

Simulation (validation scaling)

- **High-bond-dimension MERA:** benchmark $D > 8$ convergence and finite-entanglement effects on $\gamma(\tau)$.
- **Error budgets:** propagate detector-noise kernels to produce ROC-style sensitivity curves.

Experiment (near-term tests)

- **Trajectory-differentiated probes:** deploy stationary, co-moving, and accelerating detectors in BEC waterfalls; target the 10 ms–100 ms window with $\lesssim 2$ ms timing.
- **Cross-platform checks:** replicate $g^{(2)}$ envelopes in photonic-crystal and superconducting-circuit analogs.
- **Calibration:** detector-noise calibration should precede retrieval-fit attempts to ensure SNR ≥ 4 across all platforms.

Taken together, these strands converge on the same structural limit: the restoration of modular coherence under finite bandwidth. These coordinated steps will sharpen theory and enable empirical tests.

Final Remark. The split-property regularization situates ODER one layer closer to a fully rigorous Type III_1 limit within the class of Page-curve and island-based approaches. Within this operational

 doi:10.20944/preprints202503.2057.v8

framework, Type III_1 emerges as the continuum fixed point of bounded-observer modular flow, an outcome both mathematically consistent and physically measurable (see Appendix D for the explicit modular-flow fixed-point derivation). Whether confirmed or falsified, the coming analog experiments will determine whether entropy retrieval is a physical, observer-local process or merely a post-hoc bookkeeping device, marking the first empirical test of retrieval itself rather than of global entropy accounting.

Author Contributions: Conceptualization, Methodology, Software, Validation, Formal analysis, Investigation, Visualization, Writing (original draft), Writing (review and editing), Supervision, and Project administration, E.C.

Funding: This research received no external funding.

Data Availability Statement: All code, notebooks, and figure-generation scripts are archived as a single Zenodo release at https://doi.org/10.5281/zenodo.15428312 and mirrored on GitHub at https://github.com/evlocoo/ODER-modular-entropy. All materials run reproducibly in a standard Jupyter environment (without GPU acceleration) and are released under the MIT license.

- `ODER_Black_Hole_Framework_Complete_Simulation_V2.ipynb`: reproduces every figure and table in the manuscript.
- `ODER_Retrieval_Inversion_And_Validation.ipynb`: performs τ_{char} fitting, $\gamma(\tau)$ reconstruction, and validates the falsifiable $g^{(2)}(t_1, t_2)$ envelope of Lemma C.5.

Conflicts of Interest: The author declares no conflict of interest.

Appendix A. First-Principles Derivation of the Observer-Dependent Retrieval Equation

This appendix provides the formal derivation and uniqueness proofs that underwrite the retrieval law introduced in the main text; it introduces no new physical assumptions or dynamics.

All modular results below are formulated on split-regularized, finite-bandwidth subalgebras corresponding to realistic detector resolution. All entropy functions are normalized by $S_{\max}$ unless otherwise noted. **For the algebraic foundation underlying bounded modular spectra, see Appendix D.**

Theorem A.1 (Observer-Retrieval Law).

Formal underpinning of Eq. (9) in the main text.

Assumptions.

A1: a globally hyperbolic spacetime background;
A2: a faithful global state ω on the net $\mathcal{A}(O)$;
A3: an observer world line γ with wedge $D(\gamma, \tau)$;
A4: a modular spectrum bounded below.

Conclusion. The unique C^1 function $S_{\mathrm{retr}}(\tau)$ (consistent with Eq. (9)) that (i) satisfies $0 \leq S_{\mathrm{retr}} \leq S_{\max}$; (ii) is strictly increasing; (iii) obeys $\lim_{\tau\to\infty} \frac{dS_{\mathrm{retr}}}{d\tau} = 0$; and (iv) is generated by the modular automorphism group of $\mathcal{A}[D(\gamma, \tau)]$ holds:

$$\frac{dS_{\mathrm{retr}}}{d\tau} = \gamma(\tau)\left[S_{\max} - S_{\mathrm{retr}}(\tau)\right]\frac{1 + \tanh(\tau/\tau_{\mathrm{Page}})}{2}.$$

The solution is unique up to an overall scale in $\gamma(\tau)$ fixed by redshift factors and the modular-spectrum gradient.[a] □

[a] Modular operators are defined on the split-property subalgebras $\mathcal{N}_\delta$ introduced in Appendix D.

Appendix A.1. Motivation: Bounded Algebras and Observer-Dependent Entropy

Algebraic QFT assigns von Neumann algebras $\mathcal{A}(O)$ to spacetime regions O. A global state ω on $\mathcal{A}[D(\gamma, \infty)]$ encodes all degrees of freedom inside the observer's domain of dependence. At proper time τ the observer accesses only $\mathcal{A}[D(\gamma, \tau)]$; the entropy gap is the retrievable deficit.

 doi:10.20944/preprints202503.2057.v8

Finite-split regularization.

Because $\mathcal{A}(D)$ is Type III_1, its modular Hamiltonian is unbounded. A split inclusion $\mathcal{A}(D_1) \subset \mathcal{N} \subset \mathcal{A}(D_2)$ produces a Type I factor $\mathcal{N}$ with detector-bounded spectrum, preserving the Paley–Wiener condition as the split distance shrinks (Refs. [22,23]). This procedure defines the finite-bandwidth subalgebras $\mathcal{N}_\delta$ on which the bounded modular spectra $\sigma(K_\delta) \subset [-\Lambda(\delta), \Lambda(\delta)]$ are realized.

Appendix A.2. Spectral Convergence and Uniqueness of the Retrieval Sigmoid

This appendix establishes rigidity of the admissible retrieval profile under the stated analytic, spectral, and boundary assumptions, at the level required to support the physical derivations and falsifiability criteria used in the main text.

Lemma A.1 (Paley–Wiener Band-Limit). Let the split-regularized modular Hamiltonian K have bounded spectrum $\sigma(K) \subset [-\Lambda, \Lambda]$. Then any observable expectation value $f(\tau) = \langle\psi|e^{iK\tau}|\psi\rangle$, and all quantities derived from it, including the normalized entropy evolution $F(\tau) = S_{\mathrm{retr}}(\tau)/S_{\max}$, extend holomorphically to the horizontal strip

$$\mathcal{S}_\Lambda = \{\tau \in \mathbb{C} : |\Im\tau| < \pi/(2\Lambda)\},$$

with growth $|F(\tau)| = \mathcal{O}(e^{\Lambda|\Im\tau|})$. That is, F is of exponential type $\leq \Lambda$ in $\mathcal{S}_\Lambda$. (Paley–Wiener Theorem 19.3 in Rudin, *Real and Complex Analysis*). □

Lemma A.2 (Phragmén–Lindelöf Growth Bound). If $F(\tau)$ is holomorphic in $\mathcal{S}_\Lambda$, bounded and strictly monotonic on $\mathbb{R}$, and of exponential type $\leq \Lambda$, then $|F(\tau)| \leq 1$ throughout $\mathcal{S}_\Lambda$. Hence boundary monotonicity extends into the strip, excluding oscillatory band-limited variants. □

Theorem A.2 (Uniqueness of the Retrieval Sigmoid under Modular Band-Limit). Let $F : \mathbb{R} \to (0,1)$ be strictly increasing with finite limits $F(-\infty) = 0$, $F(+\infty) = 1$. Assume F satisfies Lemmas A.1–A.2. That is, it is holomorphic in $\mathcal{S}_\Lambda$, of exponential type $\leq \Lambda$, bounded on $\mathbb{R}$, and obeys the modular spectrum bound $\sigma(K) \subset [-\Lambda, \Lambda]$. Then, under these stated modular-spectral and analyticity assumptions and up to an affine reparametrization of τ,

$$\boxed{F(\tau) = \tanh\Big(\frac{\pi\Lambda}{2}(\tau - \tau_0)\Big)}.$$

Sketch of Proof. *Strip to disk map.* Map $\mathcal{S}_\Lambda$ to $\mathbb{D}$ by $z = \exp(\frac{\pi}{\Lambda}\tau)$. Define $G(\tau) = \frac{2F(\tau)-1}{2F(\tau)+1}$. Then $F(\tau) = \frac{1+G(\tau)}{1-G(\tau)}\,\frac{1}{2}$, and $G : \mathcal{S}_\Lambda \to \mathbb{D}$.

Positivity (Pick or Herglotz). Monotonicity on $\mathbb{R}$ implies $\Re[(\log\frac{1+G}{1-G})'] > 0$. That is, G is a Pick function.

Extremal solution. By Schwarz–Pick, $|G'(\tau)| \leq (\pi\Lambda/2)\,[1 - |G(\tau)|^2]$. Equality on the real axis almost everywhere forces G to be a disk automorphism, hence $G(\tau) = \tanh(\frac{\pi\Lambda}{2}(\tau - \tau_0))$.

Recover F. Undoing the Möbius transform yields the stated $F(\tau)$, with normalization $F(0) = 0$, $F(+\infty) = 1$. □

Corollary A.2.1 (Spectral Constant Fixation). The constant $(\pi\Lambda/2)$ is fixed by the strip width $|\Im\tau| < \pi/(2\Lambda)$. No other monotone analytic map satisfies both the strip bound and the modular-spectral constraint.[8]

Excluded Counterexamples.

The following functions are excluded within the stated analyticity and spectral constraints.

[8] **Paley–Wiener admissibility.** Throughout this appendix, Paley–Wiener admissibility refers to analyticity within the horizontal strip $\mathcal{S}_\Lambda = \{\tau \in \mathbb{C} : |\Im\tau| < \pi/(2\Lambda)\}$, not entire analyticity over the full complex plane.

 doi:10.20944/preprints202503.2057.v8

Candidate $F(\tau)$	**Reason for exclusion**
$(2/\pi)\arctan(\alpha\tau)$	Poles at $\pm i/\alpha$, not holomorphic in $\mathcal{S}_\Lambda$.
$1 - e^{-\alpha\tau}$	Violates strip boundedness, unbounded along $\Im\tau$.
Band-limited oscillatory sigmoids	Break strict monotonicity on $\mathbb{R}$.
Logistic $1/(1+e^{-x})$	Entire but exponential type infinite, unbounded spectrum.

These exclusions guarantee that all admissible retrieval profiles share the same analytic growth bound, ensuring that Eq. (A.2) is not merely optimal but necessary.

Physical Interpretation.

Early times ($\tau \ll \tau_{\text{char}}$) reflect incomplete activation of modular modes. Late times ($\tau \gg \tau_{\text{char}}$) approach saturation as the bounded spectrum fully enters the algebra. The tanh profile is the unique smooth analytic interpolation compatible with the Paley–Wiener bound and causal analyticity.

Diagram A.3 (Concept).

Candidate monotone curves satisfying $F(-\infty) = 0$ and $F(+\infty) = 1$. Blue, tanh, allowed. Orange, arctan, rejected due to poles. Green, exponential, rejected due to strip violation. Only the tanh profile lies within the analytic growth limits of $\mathcal{S}_\Lambda$.

Remark A.2.2 (Edge Atoms and Observer Generality).

Atomic spectral weight at $\pm\Lambda$ induces boundary oscillations incompatible with strict monotonicity on $\mathbb{R}$ and is therefore excluded by assumption. In curved or rotating backgrounds, including Kerr, the modular spectrum remains bounded after split-inclusion regularization, so the tanh onset persists. This bounded-spectrum proof generalizes to all observer classes in Section 3. The parallel with retrieval renormalization group scaling noted in Section 8 is conceptual and does not enter the present derivation.

Appendix A.3. Role of $\gamma(\tau)$: Modular Spectrum and Redshift (Parameter Interpretation)

- **Spectrum gradient:** if $\rho(\lambda) \sim \lambda^{-\beta}$, then $\gamma(\tau) \propto \tau^{\beta-1}$.
- **Geometric redshift:** stationary observers yield $\gamma_{\text{stat}} \propto 1/r$.
- **Unruh boost:** uniform acceleration gives $\gamma_{\text{acc}} \propto a^2$.

Table A1. Retrieval parameters used in numerical runs for Figures 1–2 (geometric units $G = c = 1$).

Observer	Prefactor γ_0	τ_{char}/M	τ_{Page}/M
Stationary ($r = 10M$)	0.05	8	15.0
Freely falling	0.10–0.25	4	7.5
Accelerating ($a = 0.2$)	quadratic fit	6	10.5

These prefactors correspond directly to experimentally fitted $g^{(2)}$ envelopes in Section 4, establishing traceability between algebraic and laboratory parameters.

Appendix A.4. Retrieval Saturation and Collapse Boundary

Dependency note. This proposition characterizes a boundary implied by Theorem A.1 and introduces no additional assumptions or dynamics.

Proposition A1 (Retrieval horizon τ_{RH})**.** *Let $S_{\text{retr}}(\tau)$ be the entropy-access curve derived in Theorem A.1. There exists a unique proper time τ_{RH} such that*

$$\left.\frac{d^2 S_{\text{retr}}}{d\tau^2}\right|_{\tau=\tau_{\text{RH}}} = 0, \qquad \left.\frac{d^3 S_{\text{retr}}}{d\tau^3}\right|_{\tau=\tau_{\text{RH}}} < 0.$$

 doi:10.20944/preprints202503.2057.v8

Define $\Delta_{\text{fail}} \equiv \tau_{\text{evap}} - \tau_{\text{RH}}$. *This marks the modular inflection point where retrieval curvature vanishes and saturation begins, serving as a diagnostic boundary rather than an independent evolution law.*

Appendix A.5. Observer-Bounded Automorphisms and the Origin of the tanh *Factor (Interpretive)*

Interpretive note. This subsection interprets the origin of the tanh factor already proven in Section A.2 and does not supply an independent derivation.

Theorem A.10 (below) shows that global modular flow restricts to the observer algebra and yields the unique tanh onset that appears in Eq. (9). This reflects the fact that the retrieval law saturates the Paley–Wiener bound and therefore represents the maximal causal convergence permitted by bounded modular spectra. See also Lemma A.2 for the underlying analytic constraint.

Appendix A.6. Related Work

Scope note. The works listed below address bounded algebras and entropy growth but do not derive a closed, observer-indexed retrieval law of the form used in the main text.

See Refs. [12,26,27] for parallel approaches to bounded algebras and entropy growth. These treatments likewise emphasize modular localization and spectral boundedness, though none derive a closed analytic retrieval law.

Appendix A.7. Philosophical Implications (Interpretive)

Interpretive scope. This subsection offers an interpretive reading of the retrieval law and does not introduce additional physical claims.

The law supports *relational entropy*: observer disagreements signal frame misalignment rather than information loss. In this sense, retrieval is an operational, not ontological, phenomenon; each observer accesses a bounded modular subalgebra whose growth encodes the dynamics of information recovery. This relational interpretation of entropy parallels observer-indexed coherence limits in linguistic and cosmological retrieval laws. These parallels are conceptual and are not invoked in the present derivation.

Appendix A.8. Deriving τ_{Page} *from Spectral Gaps*

Dependency note. This relation fixes the scaling of τ_{Page} rather than providing an independent definition.

With smallest modular gap $\lambda_{\min}$, $\tau_{\text{Page}} \sim \lambda_{\min}^{-1}$. For a Schwarzschild black hole of mass M, $\tau_{\text{Page}} \sim M^3$, reproducing the expected *asymptotic* semiclassical scaling of entropy-recovery timescales.

Appendix A.9. Asymptotic Boundary Clause

Boundary status. This clause defines the operational boundary of applicability of the retrieval law rather than a dynamical evolution rule.

As $\tau \to \tau_{\text{evap}} \gtrsim \tau_{\text{RH}}$, one of the following must occur: (1) $\gamma(\tau) \to 0$; (2) $S_{\max}(\tau) \to 0$; or (3) $\langle T_{\mu\nu}^{\text{retrieval}} \rangle$ becomes dynamically significant, breaking fixed-background validity. This defines the operational boundary of the ODER framework.

Remark A1 (Retrieval–Geometry Decoupling)**.** *The retrieval law holds on a fixed background and does not couple dynamically to the metric. Any extension that includes back-reaction must solve*

$$G_{\mu\nu} = 8\pi G\left(T_{\mu\nu}^{\text{Hawking}} + T_{\mu\nu}^{\text{retrieval}}\right)$$

self-consistently, which is beyond the present scope.

Empirically, only regime (3) produces observable deviation from the predicted tanh envelope. Such deviations would manifest as excess curvature in measured $g^{(2)}$ traces, marking entry into the back-reaction-dominated regime.

 doi:10.20944/preprints202503.2057.v8

Appendix A.10. Spectral Convergence and Uniqueness (Consolidation)

Consolidation note. This theorem restates the uniqueness result of Section A.2 in its spectral-limit form for completeness.

Theorem A.2 (Spectral-Convergence Constraint).
Let the split-regularized modular Hamiltonian satisfy $\sigma(K) \subset [-\Lambda, \Lambda]$. Let $F(\tau) = S_{\mathrm{retr}}(\tau)/S_{\max}$ be C^1, strictly increasing, entire, and of exponential type $\leq \Lambda$. Then, up to an affine reparameterization,

$$F(\tau) = \tanh\big(\pi\Lambda\tau/2\big).$$

Thus Eq. (9) is the only spectrum-compatible onset within the Paley–Wiener admissible class. □

This theorem subsumes the earlier Uniqueness Lemma (A.2) as its spectral-limit case, confirming consistency across analytic and modular derivations. Any smooth, monotonic retrieval profile other than tanh therefore lies outside the modularly admissible function space defined by bounded spectral support and causal analyticity. Possible generalizations would require relaxing Paley–Wiener admissibility and lie beyond the present framework.

Appendix A.11. Variational Formulation and Modular Speed Limit

Logical status. The variational formulation is logically downstream of the spectral bound and does not depend on retrieval-RG considerations.

The modular-speed-limit analysis presented here extends naturally to the finite-bandwidth formulation of Section 8, where $\Lambda(\delta) \sim 1/\delta$ defines the effective observer cutoff.

Setting and regularization.

Let $\mathcal{A}\big(D(\gamma,\tau)\big)$ be the von Neumann algebra associated with the observer's causal diamond $D(\gamma,\tau)$ along world line γ. Under the split property, the modular Hamiltonian $K(\tau)$ for $\mathcal{A}\big(D(\gamma,\tau)\big)$ admits a split-regularized spectrum $\sigma(K) \subset [-\Lambda,\Lambda]$ (Refs. [22,23]). Define the normalized retrieval profile $F(\tau) = S_{\mathrm{retr}}(\tau)/S_{\max}$. The Paley–Wiener theorem implies that F is entire of exponential type $\leq \Lambda$; its Fourier transform therefore has compact support in $[-\Lambda,\Lambda]$.

Derivative bound (Paley–Wiener/Bernstein).

For entire functions of exponential type $\leq \Lambda$, Bernstein inequalities imply $\sup_\tau |\dot{F}(\tau)| \leq \Lambda \sup_\tau |F(\tau)|$. Since $F(\tau) \in [0,1]$ is monotone and $\dot{F}(\tau) \to 0$ as $\tau \to \infty$, a tight pointwise majorant consistent with monotonicity and causal analyticity is

$$\dot{F}(\tau) \leq \Lambda[1 - F(\tau)] \tanh\Big(\tfrac{\pi\Lambda\tau}{2}\Big) =: \mathcal{B}(\Lambda,\tau), \tag{A1}$$

which defines the *modular speed limit* used in the main text.

Saturator and uniqueness (sketch).

Let $G(\tau) = \tanh\big(\frac{\pi\Lambda}{2}\tau\big)$ be the unique analytic saturator established in Section A.2. If any admissible $F(\tau)$ were to exceed the bound (A1) on a set of non-zero measure, standard Phragmén–Lindelöf and Bernstein majorant arguments for band-limited monotone maps would force violation of either the exponential-type constraint or the boundary conditions. Thus the tanh profile is the unique saturator of the modular speed limit.

Variational formulation.

The speed-limit bound admits a variational representation that reproduces the retrieval law as an Euler–Lagrange trajectory. Introduce the entropy-action functional

$$\mathcal{I}[F] = \int d\tau \Big[\tfrac{1}{2}\big(\dot{F}(\tau)\big)^2 - U\big(F;\Lambda,\tau_{\mathrm{char}}\big)\Big], \tag{A2}$$

 doi:10.20944/preprints202503.2057.v8

with potential

$$U(F;\Lambda,\tau_{\text{char}}) = \tfrac{1}{2}\Lambda^2[1-F(\tau)]^2\tanh^2\!\Big(\tfrac{\tau}{\tau_{\text{char}}}\Big). \tag{A3}$$

Because Section A.2 fixes the only analytic saturator, the extremal trajectory of (A2) is necessarily the tanh law. Stationarity yields

$$\frac{dS_{\text{retr}}}{d\tau} = \gamma(\tau)[S_{\max} - S_{\text{retr}}(\tau)]\tanh\!\Big(\tfrac{\tau}{\tau_{\text{char}}}\Big), \tag{A.2$'$}$$

coinciding with the retrieval law used in Section 2.

Onset scale τ_{char}.

When the split-regularized modular Hamiltonian exhibits a true gap $\Delta K > 0$, set

$$\tau_{\text{char}} = \frac{2\pi}{\Delta K}. \tag{A4}$$

In the generic gapless Type III_1 case, ΔK is understood as an effective spectral scale induced by the split inclusion rather than a fundamental constant.

Falsifiability.

If any measured retrieval trace violates the modular-speed-limit inequality (A1) within experimental confidence intervals, then Eq. (A.2$'$) cannot be retained as a universal observer-dependent retrieval law.

This completes the formal derivation supporting the retrieval law used throughout the main text.

Appendix B. Extended Holographic Formulation

This appendix reformulates the observer-dependent retrieval law within a holographic representation. It introduces no new dynamics and does not modify the retrieval principle established in the main text; its role is purely representational.

This appendix develops the holographic dual of the modular–retrieval framework. Observer dependence enters through the Lorentz-boost parameter Λ, which modulates both the minimal-surface geometry and the accessible modular wedge. The resulting formulation provides a covariant link between algebraic modular flow and holographic entanglement reconstruction.

Appendix B.1. Observer-Indexed Mapping to Minimal Surfaces

Definition B.1 (Observer-Indexed RT Mapping).
For a boundary subregion A and a frame boost Λ,

$$S^{\text{holo}}_{\text{obs}}(A;\Lambda) = \frac{\text{Area}[\gamma_A(\Lambda)]}{4\,G_N}\sqrt{|g_{00}(\Lambda)|}, \tag{B.1}$$

where $\gamma_A(\Lambda)$ is the codimension-2 minimal surface in the Lorentz-boosted bulk and $\sqrt{|g_{00}(\Lambda)|}$ converts boundary time to the observer's proper time. Choosing $g_{00}(\Lambda) = -1$ and $\Lambda = \mathbb{I}$ recovers the standard Hubeny–Rangamani–Takayanagi formula.

This definition encodes observer-dependent accessibility and does not replace the standard RT/HRT prescription.

Here $g_{00}(\Lambda)$ is evaluated on the boosted boundary metric, ensuring positivity of $|g_{00}|$ outside the horizon. The redshift factor is operational, not gauge, within the bounded-observer framework considered here; it excises bulk modes that remain inaccessible within the observer's proper-time flow. This explicitly aligns holographic reconstruction with the bounded modular spectra of Appendix A, ensuring that each observer's RT surface corresponds to a finite-bandwidth retrieval channel.

 doi:10.20944/preprints202503.2057.v8

Appendix B.2. Modular-Wedge Alignment and Retrieval Horizons

Dependency note. This construction geometrizes the retrieval horizon defined in Appendix A and does not introduce an independent boundary.

Let $\mathcal{W}(\Lambda)$ be the entanglement wedge reconstructed from boundary data in frame Λ. Define the retrieval horizon

$$\mathcal{R}(\Lambda) = \{\, p \in \mathcal{M}_{\text{bulk}} \mid p \in \mathcal{W}(\Lambda),\ \exists\, t \le \tau_{\text{Page}}(\Lambda) : \\ p \in \sigma_t^{\omega_\Lambda}[\mathcal{A}(A)] \,\}, \tag{A5}$$

where $\sigma_t^{\omega_\Lambda}$ is modular flow of the boosted state. The modular flow $\sigma_t^{\omega_\Lambda}$ here corresponds to the Tomita–Takesaki flow used in Theorem A.1, restricted to the holographic wedge. Retrieval saturates when $\mathcal{R}(\Lambda)$ stabilizes; its boundary $\tilde{\gamma}_A(\Lambda) \subseteq \gamma_A(\Lambda)$ marks the decodable limit.

Wedge disagreement.

If boosts Λ_1 and Λ_2 differ,

$$\gamma_A(\Lambda_1) \neq \gamma_A(\Lambda_2) \implies S_{\text{obs}}^{\text{holo}}(A;\Lambda_1) \neq S_{\text{obs}}^{\text{holo}}(A;\Lambda_2),$$

so the two observers assign different entropies to the same region, consistent with the observer-indexed trichotomy introduced in Section 7.2. The divergence between wedges provides the geometric counterpart of retrieval interference discussed in Appendix C and corresponds to the observer-class interference tensor R_{ij} introduced in Section 3.4.

Appendix B.3. Connection to HRT and Quantum Error-Correcting Codes

When the boost Λ matches the boundary slicing, Eq. (B.1) reduces to the Hubeny–Rangamani–Takayanagi prescription. In HaPPY or random-tensor MERA codes [20], the boost permutes bulk indices, changing which logical qubits are reconstructable. Our 48-qubit simulations show minimal-surface areas shifting by one MERA layer, precisely matching Eq. (B.1) and confirming that modular redshift defines the boundary–bulk retrieval channel. In network simulations, the effective redshift factor maps to layer-depth weighting: a measured shift of one MERA layer corresponds to $\Delta\tau \simeq \tau_{\text{char}}/\pi$.

Appendix B.4. Contrast with Replica Wormholes and Island Formulae

Structural contrast. The following contrast is structural rather than evaluative.

Replica-wormhole and island constructions reproduce Page-curve behavior by inserting Euclidean saddles. Equation (B.1), by contrast, achieves late-time saturation through bounded modular flow; no topology change or ensemble averaging is required. The holographic retrieval law therefore constitutes an observer-indexed Lorentzian representation of entanglement saturation, fully consistent with the algebraic modular framework of Appendix A.

Appendix B.5. Outlook

1. *Cosmological horizons:* extend Eq. (B.1) to de Sitter and FRW spacetimes, where competing boosts generate multiple retrieval horizons and entanglement wedges.
2. *Back-reaction coupling:* allow $\gamma_A(\Lambda)$ to evolve under semiclassical Einstein dynamics and study retrieval–curvature feedback linking modular flow and bulk geometry.
3. *Higher-bond-dimension networks:* test observer-dependent decoding in large-bond-dimension MERA networks to quantify how tensor geometry sets redshift factors and retrieval latency.

In synthesis, Appendices A–C establish the analytic and experimental pillars of observer-dependent retrieval, while this appendix provides a geometric realization of the same framework. Together these extensions delineate the holographic mapping regime of ODER, in which observer-indexed modular

 doi:10.20944/preprints202503.2057.v8

flow and minimal-surface reconstruction converge without introducing independent dynamics. All results in this appendix are subordinate to the retrieval law derived in the main text and Appendix A.

Appendix C. Simulation Methods and Data Analysis

This appendix documents the numerical methods and validation procedures supporting the retrieval-law derivations of Appendix A and the holographic mapping of Appendix B. All simulations implement observer-dependent modular flow within a finite-bond-dimension tensor-network proxy and are consistent with finite-bandwidth scaling; they do not constitute a numerical realization of a full retrieval-RG program.

All simulation times are expressed in geometric units ($G = c = 1$) and reported in the same M-scaled convention used in the main text, unless otherwise stated.

Appendix C.1. Simulation Setup (Methods / Validation)

Our tensor-network architecture employs a 48-qubit multiscale entanglement-renormalization ansatz (MERA) inspired by Ref. [20]. See Appendix A.11 for the analytic modular-speed-limit bound tested by these simulations. All figures in the main text derive from this geometry at bond dimension $D = 4$; an independent $D = 8$ run confirms robustness (Section C.4). The HaPPY/MERA construction is used here as a controlled, causal-cone–bounded proxy for modular flow, not as a microscopic model of black-hole degrees of freedom.

The modular wedge for each observer class is imposed by varying boundary conditions, with detector-style encodings anchoring the reconstruction depth.

Hardware envelope: All simulations ran on an Intel i7-9700 CPU (3.0 GHz, eight threads, 16 GB RAM). No GPU acceleration was required. Code and notebooks are archived on Zenodo and are reproducible in a standard Jupyter environment.

- **System architecture:** Forty-eight qubits discretize the bulk; bond edges encode holographic connectivity.
- **Initial state:** A highly entangled pure state (vacuum analog). Unitary time evolution preserves long-range correlations.
- **Boundary conditions:** Boundary tensors act as detectors and frame constraints, modified to emulate each observer class and to anchor the modular wedge.

Appendix C.2. Implementation of Observer-Dependent Channels (Methods / Validation)

- **Reconstruction regions:** Stationary observers access fixed outer layers; freely falling and accelerating observers receive time-evolving wedges that model modular growth or acceleration-induced interference.
- **Lorentz-boost encodings:** Frame-dependent boosts are applied to boundary tensors, altering reconstruction geometry and modular flow.
- **Channel variation:** Systematic wedge realignment maps directly onto the retrieval profiles of Section 3.

Appendix C.3. Data Analysis and Observable Extraction (Methods / Validation)

- **Entanglement entropy:** Successive wedges yield observer-specific Page-like curves.
- **Second-order correlation:** The simulated $g^{(2)}(t_1, t_2)$ is fit to an exponential baseline; the tanh-modulated deviation tests Eq. (13) and the retrieval law of Appendix A.
- **Parameter estimation:** Each class is sampled at 100 time points over a 500 ms window; nonlinear least squares return $\tau_{\text{retrieval}}$ and τ_{Page} with 95% confidence.

Spectral-noise amplitude was drawn from a Gaussian distribution with $\sigma \approx 0.05\,\bar{\gamma}$, ensuring bounded perturbations.

 doi:10.20944/preprints202503.2057.v8

Bootstrap procedure: Confidence bands use 200 resampled $\gamma(\tau)$ traces per class on a fixed grid with additive spectral noise (method of Section 4.1). The bond dimension scales as $D \sim \exp(L/\ell_{\mathrm{P}})$ as a tensor-network proxy; increasing D approximates deeper reconstruction layers within this numerical model, not physical AdS depth.

Appendix C.4. Discussion and Validation (Methods / Validation)

The following diagnostics verify that numerical retrieval reproduces each analytic signature derived in Appendix A and mapped geometrically in Appendix B.

- *Differential Page curves:* Entropy traces match the time-adaptive law (9).
- *Observer-modified RT surfaces:* Boundary reconstructions follow Eq. (B.1).
- $g^{(2)}$ *interference:* Accelerating observers show the predicted fringe; setting $\gamma(\tau) = 0$ removes it.
- *Bond-dimension robustness:* Doubling to $D = 8$ shifts the entropy plateau by $< 1\%$.
- *Scaling note:* Higher-bond MERA networks will probe finer reconstruction layers beyond the present 48-qubit limit within this proxy.

Appendix C.5. Falsifiable Retrieval Envelope (Falsifier)

Lemma A1 (Falsifiable $g^{(2)}$ Envelope)**.** *Let*

$$g^{(2)}(t_1, t_2) = A\left[1 - \tanh\left(\tfrac{\tau(t_1)}{\tau_{\mathrm{char}}}\right)\right]\left[1 - \tanh\left(\tfrac{\tau(t_2)}{\tau_{\mathrm{char}}}\right)\right]$$

denote the predicted envelope under bounded $\gamma(\tau)$.

Then (1) for $\gamma = 0$, $g^{(2)} \to A$ (null envelope); (2) for $\gamma(\tau) \propto 1/M$, MERA simulations reproduce retrieval collapse at τ_{RH}; (3) this structure cannot be reproduced by thermal smoothing within the bounded-observer regime unless $\gamma(\tau)$-driven curvature appears.

Thus the envelope provides a falsifiable signature of modular retrieval saturation under the stated assumptions (see also Eq. (A.2′) for the variational form).

Scope note. This lemma specifies a falsifier for the retrieval envelope within the bounded-observer framework; it does not claim uniqueness among all possible correlator structures.

Empirically, confirming deviation from the null envelope at late times requires timing resolution $\leq 2\,\mathrm{ms}$ and SNR ≥ 4, consistent with Appendix A.11 and Section 4. A complete implementation of the inversion and validation pipeline is available at https://doi.org/10.5281/zenodo.15669855. All scripts are released under an MIT license with pinned dependency versions for environment replication.

Appendix C.6. Worked Example: Macroscopic Back-Reaction (Illustrative)

Illustrative status. This worked example is provided to demonstrate scaling and order-of- magnitude suppression; it is not used elsewhere in the paper.

For a Schwarzschild black hole of mass $M = 10\,M_{\odot}$, the Bekenstein–Hawking entropy is $S_{\max} \simeq 4\pi M^2 \approx 1.5 \times 10^{78}$ (Planck units) and the horizon radius is $r_+ \simeq 30\,\mathrm{km}$. Assuming $\gamma(\tau) \sim 10^{-3}$ near τ_{RH} for accelerating observers, the retrieval stress–energy satisfies

$$\langle T_{\mu\nu}^{\mathrm{retrieval}} \rangle \sim \frac{\gamma S_{\max}}{4\pi r_+^2} \approx 1.3 \times 10^{61}\,\mathrm{m}^{-2}.$$

The Ricci tensor scales as $R_{\mu\nu} \sim 1/r_+^2 \approx 10^{-13}\,\mathrm{m}^{-2}$; restoring Planck units gives

$$\frac{G\langle T_{\mu\nu}^{\mathrm{retrieval}} \rangle}{R_{\mu\nu}} \sim 10^{-6},$$

matching the suppression bound of Section 8. Hence back-reaction remains negligible for macroscopic black holes in the parameter regime studied.

 doi:10.20944/preprints202503.2057.v8

Appendix C.7. Retrieval Interference Bound and Differential-Acceleration Interferometer (Prospective Protocol)

Overview.

This subsection defines the retrieval-interference bound $R_{ij}(\tau) \leq C(\Delta\Lambda, \tau_{\text{char}})$ and outlines a conceptual protocol for a Differential-Acceleration Interferometer (DAI). No experimental or numerical results are claimed here.

Interference-bound derivation.

Let $F_i(\tau)$ and $F_j(\tau)$ be normalized retrieval profiles for observers i and j with modular-spectrum cutoffs Λ_i and Λ_j, respectively. From Appendix A.11, each profile satisfies

$$\dot{F}_i(\tau) \leq \Lambda_i[1 - F_i(\tau)] \tanh\Big(\frac{\pi\Lambda_i\tau}{2}\Big), \tag{A6}$$

and analogously for $F_j(\tau)$.

Assuming synchronized initial conditions, define the mutual-information overlap proxy:

$$\mathcal{I}_{ij}(\tau) := \min\big(F_i(\tau), F_j(\tau)\big), \tag{A7}$$

a conservative estimator of overlap. Alternative mutual-information estimators may be substituted without altering the qualitative bound structure.

Define the retrieval-overlap tensor:

$$R_{ij}(\tau) := \frac{\mathcal{I}_{ij}(\tau)}{F_i(\tau) + F_j(\tau) - \mathcal{I}_{ij}(\tau)}. \tag{A8}$$

Let $\Delta\Lambda := |\Lambda_i - \Lambda_j|$. When $\Delta\Lambda$ is finite and onset scales differ, the overlap is bounded by

$$R_{ij}(\tau) \leq \exp\Big[-k\,\Delta\Lambda\frac{\tau^2}{\tau_{\text{char}}^2}\Big], \qquad k = \mathcal{O}(1), \tag{A9}$$

where k is a model-dependent constant determined by the overlap of the respective Paley–Wiener windows. This defines the retrieval-interference bound $C(\Delta\Lambda, \tau_{\text{char}})$.

Null envelope.

The null model assumes $\gamma(\tau) = 0$, corresponding to thermal drift or decoherence with no modular retrieval. Baseline envelopes $R_{ij}^{(\text{null})}(\tau)$ are estimated from bootstrap-generated retrieval traces lacking observer-indexed structure.

ROC-style comparison.

Measured $R_{ij}(\tau)$ can be compared to a null envelope via:

- **True positive:** $R_{ij}(\tau) < R_{ij}^{(\text{null})}(\tau) - 3\sigma$ at any τ;
- **False positive:** a null trace misclassified as divergent.

A ROC curve is then constructed by varying the detection threshold. Simulated ROC curves used $N = 10^3$ bootstrap samples; empirical verification would require differential-arm timing precision $\leq 2\,\text{ms}$ and fringe stability $> 95\%$. This approach parallels the falsifiability criterion of the $g^{(2)}$ envelope (Appendix A.11, Eq. (A.2′)).

Conceptual DAI protocol.

In a conceptual DAI setup using a BEC analog system:

- Stationary and accelerated detector arms are phase-locked at $\tau = 0$;
- Each arm samples its local phonon field and extracts $g^{(2)}(t_1, t_2)$;
- Retrieval curves are reconstructed via entropy-constrained filtering;

 doi:10.20944/preprints202503.2057.v8

- A thermal null model is generated by disabling modular coupling.

These derivations clarify what empirical retrieval divergence would look like under the ODER framework. No specific experiment or simulation is assumed to have been completed.

Appendix C.8. Modular Raychaudhuri Equation (Exploratory Extension)

Exploratory status. This subsection is an exploratory extension and is not used in the main text or in any validation claim.

Equations (A.2′) and (C.24) jointly motivate this coupling: the same retrieval curvature that bounds modular speed now sources modular expansion.

In all preceding sections, retrieval dynamics were modeled under a fixed-background approximation. We now extend the framework by coupling entropy retrieval to spacetime curvature through a modular analogue of the Raychaudhuri equation. This introduces a dynamical back-reaction term sourced by the entropy-convergence profile $S_{\text{retr}}(\tau)$, allowing retrieval to both track and influence horizon geometry.

Modular expansion scalar.

Define the modular expansion $\theta_{\text{mod}}(\tau)$ as the divergence of modular-flow lines weighted by the retrieval gradient:

$$\theta_{\text{mod}}(\tau) \equiv \nabla_\mu u^\mu + \alpha \frac{dS_{\text{retr}}}{d\tau},$$

where u^μ is the observer's four-velocity and $\alpha \ll 1$ is the retrieval-coupling parameter introduced in Section 8.

Modular Raychaudhuri equation.

The modular analogue of the Raychaudhuri equation takes the form

$$\frac{d\theta_{\text{mod}}}{d\tau} = -\tfrac{1}{2}\theta_{\text{mod}}^2 - \sigma_{\mu\nu}\sigma^{\mu\nu} + \omega_{\mu\nu}\omega^{\mu\nu} - R_{\mu\nu}u^\mu u^\nu + \alpha \frac{d^2 S_{\text{retr}}}{d\tau^2},$$

where $\sigma_{\mu\nu}$ and $\omega_{\mu\nu}$ are the shear and vorticity tensors of the modular-flow congruence, and $R_{\mu\nu}$ is the Ricci tensor. Metric signature follows $(-,+,+,+)$; $R_{\mu\nu}u^\mu u^\nu > 0$ corresponds to focusing. The term $\alpha\, d^2 S_{\text{retr}}/d\tau^2$ acts as a retrieval-driven focusing or defocusing force: when retrieval accelerates (positive second derivative) it produces modular expansion; when retrieval saturates or decelerates, curvature focusing dominates.

Limiting behavior.

In the limit $\alpha \to 0$, this reduces to the standard Raychaudhuri equation in a fixed background, recovering geodesic congruence evolution. Thus the modular extension preserves classical behavior in the retrieval-free case.

Back-reaction shift.

To leading order in α, the retrieval horizon τ_{RH} shifts by

$$\delta\tau_{\text{RH}} \sim \alpha \int^{\tau_{\text{RH}}} d\tau' \Big(\frac{d^2 S_{\text{retr}}}{d\tau'^2} \Big),$$

and numerical estimates (Appendix C.9) indicate this shift remains negligible for $M \gtrsim M_\odot$ but may become resolvable in analog systems with boosted retrieval rates. In such analog systems, a non-zero α would manifest as a slow drift of the measured τ_{RH} across successive retrieval cycles.

 doi:10.20944/preprints202503.2057.v8

Interpretation.

The modular Raychaudhuri equation operationalizes the idea that entropy retrieval is not merely a diagnostic of black-hole evaporation but can itself act as a geometric source. Failure of monotonic convergence in $S_{\text{retr}}(\tau)$ signals not only information-theoretic breakdown but potential modular collapse. In this sense, the retrieval law and the modular flow it induces are not spectators to geometry; they are participants in its evolution.

Appendix C.9. Modular Focusing and the Retrieval–Curvature Coupling (Exploratory Extension)

Exploratory status. This section elaborates the modular Raychaudhuri construction as a possible future extension. It introduces no new constraints on the retrieval law and is not required for any result in the main text.

Setup.

Let u^μ be the observer's proper-time tangent vector, and let $\theta(\tau) = \nabla_\mu u^\mu$ denote the expansion of the modular flow congruence. The retrieval-coupled expansion scalar is defined as

$$\theta_{\text{mod}}(\tau) = \theta(\tau) + \alpha \frac{dS_{\text{retr}}}{d\tau}.$$

Modular-congruence evolution.

Taking the τ-derivative yields

$$\frac{d\theta_{\text{mod}}}{d\tau} = \frac{d\theta}{d\tau} + \alpha \frac{d^2 S_{\text{retr}}}{d\tau^2}.$$

Inserting the classical Raychaudhuri equation,

$$\frac{d\theta}{d\tau} = -\tfrac{1}{2}\theta^2 - \sigma_{\mu\nu}\sigma^{\mu\nu} + \omega_{\mu\nu}\omega^{\mu\nu} - R_{\mu\nu}u^\mu u^\nu,$$

we obtain the modular-coupled version

$$\frac{d\theta_{\text{mod}}}{d\tau} = -\tfrac{1}{2}\theta_{\text{mod}}^2 - \sigma_{\mu\nu}\sigma^{\mu\nu} + \omega_{\mu\nu}\omega^{\mu\nu} - R_{\mu\nu}u^\mu u^\nu + \alpha \frac{d^2 S_{\text{retr}}}{d\tau^2} + \mathcal{O}(\alpha^2).$$

The θ_{mod}^2 term absorbs the linear α correction to θ, while all other terms remain unaffected at first order.

Horizon shift.

The retrieval horizon τ_{RH} is defined as the proper time at which $S_{\text{retr}}(\tau) \to S_{\max}$. To leading order in α,

$$\delta\tau_{\text{RH}} = \alpha \int_0^{\tau_{\text{RH}}} \frac{d^2 S_{\text{retr}}}{d\tau^2}\, d\tau.$$

This integral can be evaluated analytically for constant-γ tanh models or numerically using retrieval simulations.

Remarks.

This derivation assumes modular flow remains smooth and geodesic at leading order. Future work may incorporate non-affine corrections, edge-mode interactions, or observer switching. The modular Raychaudhuri equation defines a new class of entropy-coupled geometric dynamics. Where $S_{\text{retr}}(\tau)$ is highly nonlinear—for example, under interference, collapse, or multi-observer divergence— θ_{mod} may blow up, indicating modular-horizon instability. This provides a structural falsifier: monotonic retrieval convergence is required to prevent runaway geometric focusing.

 doi:10.20944/preprints202503.2057.v8

In this view, modular flow, retrieval dynamics, and curvature evolution form a coupled triad. This perspective is presented as a possible extension rather than as a claim of completed dynamics.

Appendix D. Split-Property Regularization and the Type III_1 Limit

This appendix specifies the mathematical regularization that renders observer-dependent retrieval well defined and delineates the formal boundary between finite-observer physics and the Type III_1 continuum idealization.

Local algebras in algebraic quantum field theory (AQFT) are generically Type III_1 factors: they possess no normal trace and therefore admit no literal density matrix or entropy functional. To formulate observer-dependent entropy retrieval within a physically meaningful regime, we employ the standard *split-property regularization* used in rigorous AQFT treatments of entropy and modular flow.

Appendix D.1. Split Inclusion and Bounded Modular Spectrum (Formal Construction)

Following standard split-property constructions in AQFT [23–25], we introduce nested regions $O_1 \subset O_2$ and a Type I intermediate factor: we introduce nested regions $O_1 \subset O_2$ and a Type I intermediate factor:

$$\mathcal{A}(O_1) \subset \mathcal{N}_\delta \subset \mathcal{A}(O_2),$$

where the split distance δ defines the physical collar between the inner and outer regions. The modular Hamiltonian K_δ generated by the state ω on $\mathcal{N}_\delta$ then has a compact spectrum,

$$\sigma(K_\delta) \subset [-\Lambda(\delta), \Lambda(\delta)] \quad \text{(bounded in operator norm; } |K_\delta| \leq \Lambda(\delta)).$$

This provides a well-defined finite entropy and modular flow. Operationally, δ corresponds to the detector's spatial or temporal resolution, and $\Lambda(\delta) \sim 1/\delta$ represents the associated bandwidth limit.

Appendix D.2. Physical Interpretation (Operational Interpretation)

Real observers cannot access modes beyond their finite bandwidth; the split inclusion therefore captures the physically retrievable subalgebra of the full theory. All bounded-spectrum statements in this work refer to such operationally defined $\mathcal{N}_\delta$. In the limit $\delta \to 0$, $\Lambda(\delta) \to \infty$ and the algebra returns to the Type III_1 class. Within the regulated regime, the modular-flow retrieval law derived in the main text (Eq. (9)) is exact; the Type III_1 limit marks the idealized boundary where observer bandwidth becomes infinite.

Appendix D.3. Connection to the Retrieval–RG Picture (Interpretive Correspondence)

Define the retrieval-renormalization parameter:

$$\beta_\Lambda(\delta) = \frac{d \ln \Lambda(\delta)}{d \ln \delta}.$$

The Type III_1 structure corresponds to the fixed point $\beta_\Lambda \to 0$, signaling scale-invariant modular spectra. Finite observers operate at $\beta_\Lambda < 0$, where the spectrum is effectively bounded and the tanh retrieval law applies directly.

This establishes an interpretive renormalization-group analogue of the split-property hierarchy: as the split collar narrows, the modular spectrum flows toward the continuum fixed point. This renormalization-group analogy is descriptive and does not generate the retrieval law, which is fixed independently by modular analyticity and bounded spectra. In laboratory analogs, varying detector resolution δ directly probes this correspondence: retrieval parameters should approach $\beta_\Lambda \approx 0$ as experimental bandwidth increases.

 doi:10.20944/preprints202503.2057.v8

Appendix D.4. Scope and Open Formal Problems (Open Formal Problems)

Here Δ_δ^{it} denotes the modular automorphism group generated by K_δ. This regularization does not purport to solve the Type III_1 classification problem; it provides a physically covariant framework in which finite observers are well defined. The continuum Type III_1 limit remains a mathematical frontier. Future work should formalize:

1. the weak-operator convergence $\Delta_\delta^{it} \to \Delta^{it}$ of modular flows;
2. conditions under which isotony and locality persist for the directed family $\{\mathcal{N}_\delta\}$; and
3. quantitative scaling of $\rho_\delta(\lambda)$ approaching the Type III_1 fixed point.

Bridging these mathematical results with the retrieval–RG framework of Section 8 would complete the formal connection between bounded modular spectra and scale-invariant entropy flow.

Appendix D.5. Physical Meaning of the Type III_1 Limit (Interpretive Limit)

As discussed in Appendix A.7, relational entropy interprets this limit not as loss of information but as the restoration of scale-invariant modular access. In algebraic QFT, Type III_1 algebras are the unique structures compatible with relativistic locality and causal propagation: they admit no finite trace and thus no factorization between interior and exterior regions. "Inevitable" here refers to the continuum idealization of finite-observer regularizations, not to an operationally accessible physical regime.

Within the retrieval–RG picture, increasing observer bandwidth ($\delta \to 0$) drives the modular spectrum toward scale invariance, the Type III_1 fixed point of bounded-observer modular flow. Real detectors operate at finite δ; the continuum theory represents the unphysical ideal of infinite information access.

All physical predictions in this work are confined to finite δ; the Type III_1 limit functions solely as the formal boundary of the theory.

Appendix E. Modular Retrieval in Kerr Geometry: Generator Deformation and Spectral Persistence

This appendix tests the stability of the retrieval law under stationary generator deformation in Kerr geometry. It introduces no new dynamics and relies only on assumptions already established in the main text and Appendix A.

Appendix E.1. Kerr Geometry and Modular Flow (Geometric Setup)

In Kerr spacetime the global timelike Killing vector ∂_t is replaced by a stationary, non-static modular generator,

$$\chi^\mu = \partial_t + \Omega_H \, \partial_\phi,$$

where Ω_H is the horizon angular velocity. Modular flow follows the mixed time–angle trajectory generated by χ^μ; an observer therefore does not evolve on a globally synchronized slice. The modular Hamiltonian K_χ associated with this generator defines observer-adapted modular flow consistent with the split-property regularization described in Appendix D.

Appendix E.2. Modular-Generator Deformation (Generator Deformation and Spectral Admissibility)

Because the modular Hamiltonian depends linearly on the generator, the deformation $(\partial_t \to \chi^\mu)$ preserves the Paley–Wiener class of admissible modular flows. This preservation concerns spectral admissibility of modular evolution, not dynamical stability of the Kerr spacetime itself. Anchoring the causal diamond to χ^μ yields a Kerr-corrected retrieval rate,

$$\gamma(\tau, a, \Omega_H) = |g_{\mu\nu}\chi^\mu\chi^\nu|^{-1/2},$$

 doi:10.20944/preprints202503.2057.v8

which captures frame dragging and horizon-synchronous motion. In rotating BEC analogs, frame dragging corresponds to azimuthal phonon flow; measuring the resulting $g^{(2)}$ phase shift tests Eq. (A10).

Appendix E.3. Survival of the tanh *Onset (Stability Result)*

For observers outside the ergoregion ($r > r_{\text{erg}}$) the modular spectrum remains bounded after split-inclusion regularization. The Paley–Wiener conditions therefore still hold, and the retrieval law,

$$\frac{dS_{\text{retr}}}{d\tau} = \gamma(\tau, a, \Omega_H)[S_{\max} - S_{\text{retr}}(\tau)] \tanh\big(\tau/\tau_{\text{char}}\big), \tag{A10}$$

retains its form; rotation deforms the horizon but does not disrupt modular convergence. This persistence confirms that the tanh onset derived in Appendix A.2 is not restricted to static geometries. *Units adopt* $G = c = \hbar = 1$ and metric signature $(-,+,+,+)$; under this convention, $|g_{\mu\nu}\chi^\mu\chi^\nu|$ is positive outside the horizon.

Appendix E.4. Superradiance and Spectral Containment (Domain Restriction)

Superradiant amplification in Kerr is energy dependent and frame relative. Modular spectral weight remains bounded provided (i) the observer remains outside the ergosphere and (ii) detector resolution imposes a UV cutoff (Appendix A.3). Under these conditions the retrieval wedge remains modularly coherent, and the Paley–Wiener analyticity domain remains intact. Behavior inside the ergoregion lies outside the bounded-observer regime considered here and is not addressed by the present analysis.

Appendix E.5. Interpretation and Consequences (Interpretive Consequences)

- The tanh onset is *not* an artifact of Schwarzschild symmetry; it is a feature of bounded modular spectra.
- Modular retrieval is geometrically robust: Kerr rotation modulates $\gamma(\tau)$ but preserves spectral convergence.
- The retrieval law is covariant under stationary generator deformation within the regular wedge class.

Conclusion. Conclusion. Modular retrieval survives Kerr rotation. Persistence of Eq. (A10) under stationary generator deformation demonstrates robustness of the retrieval law across stationary spacetimes with bounded modular spectra. This result establishes stability under rotation without extending the domain of validity beyond observer-bounded regimes or invoking new dynamics.

Appendix F. Interpretive Correspondence (Non-Essential)

Readers seeking only the formal modular derivations may skip this appendix. It translates ODER's algebraic parameters into gravitational and holographic language for conceptual cross-reference. All quantities retain their definitions from Appendices A and D; the equations below are interpretive analogies, not additional postulates.

Although the ODER retrieval law is derived entirely from observer-dependent modular flow, several of its structural parameters parallel gravitational constructs familiar from wedge-based approaches to the black-hole information problem. The correspondences below serve as interpretive aids for readers who work primarily with holography or extremal-surface reconstruction.

Appendix F.1. Bandwidth and Algebraic Context

The variables δ and $\Lambda(\delta)$ introduced in Appendix D connect the modular-algebraic description to measurable observer parameters. Finite δ defines the retrievable subalgebra $\mathcal{N}_\delta$ with spectral cutoff $\Lambda(\delta) \sim 1/\delta$; the continuum limit $\delta \to 0$ recovers the Type III_1 structure of AQFT. This identification grounds the analytic variables of ODER in the algebraic foundations of relativistic QFT without altering their physical interpretation elsewhere in the framework.

 doi:10.20944/preprints202503.2057.v8

Appendix F.2. Interpretive Parameter Correspondence

Each correspondence below references the bounded-spectrum formalism of Appendix A.11 and the retrieval-RG scaling of Sec. 8.

- Δ_{fail} **(failure gap).** In ODER, $\Delta_{\text{fail}} \equiv \tau_{\text{evap}} - \tau_{\text{RH}}$ represents the late-stage failure of entanglement-wedge reconstruction, where extremal surfaces no longer support modular access for the observer's causal patch. Mathematically this corresponds to the vanishing of the second derivative $d^2 S_{\text{retr}}/d\tau^2$ at the retrieval horizon τ_{RH}. ODER treats this as a retrieval-saturation condition—a collapse of spectral access governed by observer-specific modular flow rather than by global extremal anchoring.
- τ_{char} **(convergence time).** The modular convergence scale that marks the start of retrieval serves as a spectrally modulated scrambling threshold. Conventional scrambling time signals full entanglement redistribution, whereas τ_{char} emerges from bounded modular flow and captures observer-relative retrieval activation even when causal connectivity exists but modular access is still suppressed. Experimentally it governs the width of the measured $g^{(2)}$ envelope (Sec. 4.1).
- $\gamma(\tau)$ **(retrieval operator).** Derived from the entropy trace, $\gamma(\tau)$ measures the local modular pressure—the instantaneous rate at which retrievable entropy moves toward saturation. Within the modular algebra, $\gamma(\tau)$ appears as the local generator of the positive-energy semigroup for the observer's subalgebra $\mathcal{N}_\delta$. A gravitational analogue would be a time-dependent coupling between boundary modular flow and evolving bulk extremal surfaces. Because $\gamma(\tau)$ varies smoothly with both trajectory and state, it serves as an information-theoretic redshift gradient tied to curvature of the modular spectrum.

These mappings are interpretive guides, not theoretical requirements. The ODER retrieval law is complete within modular-flow formalism and requires no holographic embedding. Causal wedges and HRT surfaces offer intuitive parallels, but they are projections of the same underlying modular dynamics rather than foundations. A full gravitational embedding is deferred to future work and is included here only to aid conceptual translation.

Appendix F.3. Extended Variable Glossary (Table F.1)

Symbol	Description	Interpretation	Experimental / Simulation Proxy
δ	Split-property collar / detector resolution	Physical bandwidth of the observer; defines the retrievable subalgebra	—
$\Lambda(\delta)$	Modular spectral cutoff	Inverse bandwidth ($\Lambda \sim 1/\delta$); controls the tanh prefactor and approach to the Type III_1 limit	—
τ_{char}	Convergence (activation) time	Onset scale of modular retrieval; analog of a scrambling threshold	Width of $g^{(2)}$ transition
Δ_{fail}	Retrieval-failure gap	Proper-time delay between evaporation and saturation limits	Duration between entropy plateau and null-envelope flattening
$\gamma(\tau)$	Retrieval-rate operator	Local modular pressure or information-flux density	Slope of entropy-retrieval trace

 doi:10.20944/preprints202503.2057.v8

Appendix F.4. Cross-Domain Interpretive Map (Table F.2)

Term	Physics Interpretation	Algebra / AQFT Interpretation
Modular flow	Local observer evolution in proper time; defines trajectory of modular access	Tomita–Takesaki automorphism on $\mathcal{A}(O)$ governing modular evolution
Retrieval horizon	Boundary of the decodable information wedge for a given observer	Support boundary of the retrievable subalgebra $\mathcal{N}_\delta$
Type III_1 fixed point	Scale-invariant modular spectrum; continuum limit of retrieval flow	Non-factorizable local algebra; no trace; required by Haag–Kastler locality axioms

Summary. The interpretive correspondences collected here are heuristic aids for cross-domain intuition. They situate the modular parameters of ODER within the gravitational vocabulary of wedges, surfaces, and bandwidths without requiring any holographic assumption. Finite-bandwidth retrieval, its modular-algebraic foundations, and its covariant persistence across geometries jointly establish ODER as a first-principles description of observer-dependent entropy flow.

References

1. Almheiri, A.; Engelhardt, N.; Marolf, D.; Maxfield, H. The Entropy of Bulk Quantum Fields and the Entanglement Wedge of an Evaporating Black Hole. *J. High Energy Phys.* **2019**, 063. https://doi.org/10.1007/JHEP12(2019)063
2. Penington, G.; Shenker, S.H.; Stanford, D.; Yang, Z. Replica Wormholes and the Black Hole Interior. *Phys. Rev. D* **2021**, *103*, 084007. https://doi.org/10.1103/PhysRevD.103.084007 [*arXiv*:1911.11977 (hep-th)]
3. Almheiri, A.; Hartman, T.; Maldacena, J.; Shaghoulian, E.; Tajdini, A. The Entropy of Hawking Radiation. *Rev. Mod. Phys.* **2021**, *93*, 035002. https://doi.org/10.1103/RevModPhys.93.035002
4. Liu, H.; Vardhan, S. Entanglement Entropies of Equilibrated Pure States in Quantum Many-Body Systems and Gravity. *PRX Quantum* **2021**, *2*, 010344. https://doi.org/10.1103/PRXQuantum.2.010344
5. Page, D.N. Average Entropy of a Subsystem. *Phys. Rev. Lett.* **1993**, *71*, 1291–1294. https://doi.org/10.1103/PhysRevLett.71.1291
6. Hayden, P.; Preskill, J. Black Holes as Mirrors: Quantum Information in Random Subsystems. *J. High Energy Phys.* **2007**, 120. https://doi.org/10.1088/1126-6708/2007/09/120
7. Jafferis, D.L.; Bluvstein, D.; Himmelspach, M.; et al. Traversable Wormhole Dynamics on a Quantum Processor. *Nature* **2022**, *612*, 51–55. https://doi.org/10.1038/s41586-022-05424-3
8. Astesiano, D.; Gautason, F.F. Supersymmetric Wormholes in String Theory. *Phys. Rev. Lett.* **2024**, *132*, 161601. https://doi.org/10.1103/PhysRevLett.132.161601
9. Akers, C.; Faulkner, T.; Lin, S.; Rath, P. The Page Curve for Reflected Entropy. *J. High Energy Phys.* **2022**, *06*, 089. https://doi.org/10.1007/JHEP06(2022)089
10. Brunetti, R.; Fredenhagen, K.; Verch, R. The Generally Covariant Locality Principle: A New Paradigm for Local Quantum Field Theory. *Commun. Math. Phys.* **2003**, *237*, 31–68. https://doi.org/10.1007/s00220-003-0815-7
11. Witten, E. APS Medal for Exceptional Achievement in Research: Entanglement Properties of Quantum Field Theory. *Rev. Mod. Phys.* **2018**, *90*, 045003. https://doi.org/10.1103/RevModPhys.90.045003
12. Chandrasekaran, V.; Longo, R.; Penington, G.; Witten, E. An Algebra of Observables for de Sitter Space. *J. High Energy Phys.* **2023**, 082. https://doi.org/10.1007/JHEP02(2023)082
13. Crispino, L.C.B.; Higuchi, A.; Matsas, G.E.A. The Unruh Effect and Its Applications. *Rev. Mod. Phys.* **2008**, *80*, 787–838. https://doi.org/10.1103/RevModPhys.80.787
14. Steinhauer, J. Observation of Quantum Hawking Radiation and Its Entanglement in an Analogue Black Hole. *Nat. Phys.* **2016**, *12*, 959–965. https://doi.org/10.1038/nphys3863
15. Casini, H.; Huerta, M.; Myers, R.C. Towards a Derivation of Holographic Entanglement Entropy. *J. High Energy Phys.* **2011**, 036. https://doi.org/10.1007/JHEP05(2011)036
16. Dong, X.; Harlow, D.; Wall, A.C. Reconstruction of Bulk Operators within the Entanglement Wedge. *Phys. Rev. Lett.* **2016**, *117*, 021601. https://doi.org/10.1103/PhysRevLett.117.021601
17. Casini, H.; Teste, E.; Torroba, G. Modular Hamiltonians on the Null Plane and the Markov Property of the Vacuum State. *J. Phys. A: Math. Theor.* **50**, 364001 (2017). https://doi.org/10.1088/1751-8121/aa7eaa

 doi:10.20944/preprints202503.2057.v8

18. Jafferis, D.L.; Lewkowycz, A.; Maldacena, J.; Suh, S.J. Relative Entropy Equals Bulk Relative Entropy. *J. High Energy Phys.* **2016**, 004. https://doi.org/10.1007/JHEP06(2016)004
19. Faulkner, T.; Li, M. Asymptotically Isometric Codes for Holography. *arXiv* **2022**, arXiv:2211.12439 [hep-th]. https://doi.org/10.48550/arXiv.2211.12439
20. Pastawski, F.; Yoshida, B.; Harlow, D.; Preskill, J. Holographic Quantum Error-Correcting Codes: Toy Models for the Bulk/Boundary Correspondence. *J. High Energy Phys.* **2015**, 149. https://doi.org/10.1007/JHEP06(2015)149
21. York, J.W., Jr. Black Hole in Thermal Equilibrium with a Scalar Field: The Back-Reaction. *Phys. Rev. D* **1985**, *31*, 775–784. https://doi.org/10.1103/PhysRevD.31.775
22. Casini, H.; Huerta, M.; Rosabal, J.A. Remarks on Entanglement Entropy for Gauge Fields. *Phys. Rev. D* **2014**, *89*, 085012. https://doi.org/10.1103/PhysRevD.89.085012
23. D'Antoni, C.; Longo, R. Interpolation by Type I Factors and the Flip Automorphism. *J. Funct. Anal.* **2001**, *182*, 367–385. https://doi.org/10.1006/jfan.2000.3744
24. Longo, R. Notes on Algebraic Invariants for Noncommutative Dynamical Systems. *Commun. Math. Phys.* **1979**, *69*, 195–207. https://doi.org/10.1007/BF01197443
25. Araki, H. Relative Entropy for States of von Neumann Algebras II. *Publ. Res. Inst. Math. Sci.* **1977**, *13*(1), 173–192. https://doi.org/10.2977/prims/1195190105
26. Witten, E. Gravity and the Crossed Product. *J. High Energy Phys.* **2022**, 008. https://doi.org/10.1007/JHEP10(2022)008
27. Srednicki, M. Chaos and Quantum Thermalization. *Phys. Rev. E* **1994**, *50*, 888–901. https://doi.org/10.1103/PhysRevE.50.888
28. Almheiri, A.; Marolf, D.; Polchinski, J.; Sully, J. Black Holes: Complementarity or Firewalls? *J. High Energy Phys.* **2013**, 062. https://doi.org/10.1007/JHEP02(2013)062
29. Castro, A.; Maloney, A.; Strominger, A. Hidden Conformal Symmetry of the Kerr Black Hole. *Phys. Rev. D* **2010**, *82*, 024008. https://doi.org/10.1103/PhysRevD.82.024008
30. Takesaki, M. *Tomita's Theory of Modular Hilbert Algebras and Its Applications*. Springer: Berlin, 1970. https://doi.org/10.1007/BFb0059704
31. Maldacena, J.; Susskind, L. Cool Horizons for Entangled Black Holes. *Fortschr. Phys.* **2013**, *61*, 781–811. https://doi.org/10.1002/prop.201300020
32. Ryu, S.; Takayanagi, T. Holographic Derivation of Entanglement Entropy from AdS/CFT. *Phys. Rev. Lett.* **2006**, *96*, 181602. https://doi.org/10.1103/PhysRevLett.96.181602
33. Jacobson, T. Thermodynamics of Spacetime: The Einstein Equation of State. *Phys. Rev. Lett.* **1995**, *75*, 1260–1263. https://doi.org/10.1103/PhysRevLett.75.1260
34. Martirosyan, G.; Gazo, M.; Etrych, J.; *et al.* A universal speed limit for spreading of coherence. *Nature* **2025**, *647*, 608–612. https://doi.org/10.1038/s41586-025-09735-z
35. Rudin, W. *Real and Complex Analysis*, 3rd ed. McGraw–Hill: New York, 1987.